Honors Thesis

Zinc's impact on triple-negative breast cancer: investigating cell viability and apoptosis

Alyx Lanthier

Department of Biochemistry

9 April 2025

Thesis Advisor: Dr. Amy Palmer (Department of Biochemistry)

Committee Members: Dr. Joseph Falke (Department of Biochemistry) & Dr. Jihye Park (Department of Chemistry)

University of Colorado, Boulder

Spring 2025

Contents

Abstract

Zinc has been shown to play a major role in maintaining the health of a living organism through proper enzymatic function, growth and development, and gene regulation. However, until recently there was little information on the effects of zinc on apoptosis in epithelial breast cells. Results from the live/dead assays performed on two TNBC cell lines (MDA-MB-231 and MDA-MB-157) compared to a healthy epithelial breast cell line (MCF10A) provided important findings with respect to the viability of TNBC cell lines when treated in zinc-deficient conditions. Interested in the mechanism of cell death observed from the live/dead assay results on the MDA-MB-231 cells treated to zinc-deficient conditions and MCF10A cells treated to zinc-rich conditions, apoptosis assays were performed on these cells following similar zinc treatments. Although further optimization of the assay is required, current data provides important insight into the mechanism of death observed in these cell lines. Overall, the live/dead and apoptosis assays suggest that TNBCs have a strong dependency on zinc, and without it, they become both necrotic and apoptotic, whereas zinc-rich conditions induce mainly apoptosis in healthy epithelial breast cells.

---------- Introduction ----------

What is Cancer?

i. A brief statistic

In 2022, 20 million new cases of cancer were diagnosed worldwide and nearly 10 million people died from this disease (National Cancer Institute, 2024). The rise in new cases each year, along with the rise in mortality rate, are the main drivers to better characterize cancers and thus develop new therapeutic strategies to tackle them. This has proven effective as there were around 18 million cancer survivors in the U.S. alone, and an estimated rise of about 5 million yearly survivors by 2032 (National Cancer Institute, 2024). However, this issue is proving difficult to tackle and it starts with understanding what cancer is.

ii. Importance of context

Cancer, in short, is an accumulation of cell abnormalities that renders the cell immortal. On average, the number of these abnormalities ranges from 2 to 8 depending on the type of cancer (Anandakrishnan et al., 2019). A more scientifically accepted word for describing these abnormalities would be *mutations*. To better understand cancer, it is essential to first consider some foundational biological context.

The average human body contains an estimated 30 trillion cells (Sender et al., 2016). This is thousands of times larger than the number of people walking on this planet today. Imagining everyone on earth working together in harmony would be nearly impossible. However, cells do not consciously choose to work together, they just happened to evolve this way over billions of

years (Libby & Ratcliff, 2014). It may be hard to imagine at first, but cells function on the basis of random molecular interactions, unlike humans who make conscious choices in their lives. Some of these random interactions proved more favorable than others, shaping the diversity of cells seen in life today. In the context of this paper on human cells, it's important to consider that the random events that led to these trillions of cells working together can still be described as *mutations*.

iii. Importance of perspective

Whether a mutation is 'good' or 'bad' can be hard to determine without perspective; the organism and the environment it lives in. Some mutations can increase the overall survivability of an organism. For example, it is suggested that the ability to digest lactose as an adult is a mutation that increased the expression of lactase, an enzyme required to break down lactose, and became prevalent in societies that relied on milk consumption (Swallow, 2003). On the other hand, some mutations can decrease overall survivability, much like cancer in humans. However, from the perspective of the cancer cell, it actually seems to be thriving from these mutations, so much so that cancer cells are often described to be immortalized (Hayflick & Moorhead, 1961). Depending on the perspective there seems to be intent behind these mutations. In the case of lactose tolerance, became prevalent in societies that rely on dairy consumption, and in the case of cancer cells, the cells become immortal. On the surface, it would appear that there are clear reasons for these mutations to occur, nonrandomly.

To understand the randomness of mutations, it's best to take a look at what's happening from a molecular view. The 'central dogma of biology' is a term coined by Francis Crick in the mid to late 20th century. It describes the natural order of cellular function at the molecular level: DNA (deoxyribonucleic acid) is transcribed into RNA (ribonucleic acid) which is then translated into proteins that carry out most functions within a cell (Crick, 1970). Some of the most important functions of these proteins govern when and how a cell will divide, analogous to a human's survivability and reproducibility. The randomness of these mutations comes into play during the cell cycle, more specifically the proteins that govern how a cell divides.

The cell cycle can be split into many subdivisions, G_0, G_1, S, G_2, and a mitotic M phase (Alberts et al., 1994). For the context of defining cancer, the S phase is a good starting point. This is because, during the S phase, DNA is replicated, as every cell needs its own copy of DNA. Knowing that every multi-cellular organism originated from a single cell, in a perfect world, every cell in said organism should then share an identical genome. This is not the case. The reason is that one of the various proteins that governs how a cell divides is the DNA polymerase, which is not perfect. As many may know, DNA is double-stranded and comprised of 4 nitrogenous bases; A (adenine), T (thymine), G (guanine), and C (cytosine), where A pairs with T and G pairs with C, also known as Watson-Crick base pairing (Watson & Crick, 1953). This means that it is the DNA polymerase's job to replicate the DNA by correctly pairing these bases with new ones, but on average it makes a mistake once every billion base pairs (Drake et al., 1998). The length of the average human's genome is 3 billion base pairs, so with each round of DNA replication, the newly replicated genome could differ by around 3 base pairs. This process is what makes a mutation random.

It's not that drinking milk as an adult causes the body to produce more lactase in response. Instead, individuals who randomly acquired this mutation gained a 'fitness advantage' in societies that relied on milk consumption for survival. Similarly, a cancer cell does not develop mutations in response to external factors with the goal of becoming immortal. Rather, cancer arises when random mutations---some of which happen to be advantageous---allow the cell to out-survive its peers. If these mutations were not beneficial for survival, the cancerous cells would not persist, just as lactose tolerance would not have spread in populations without dairy consumption, yet some individuals would still produce more lactase than others.

iv. Defining hallmarks

Understanding that the significance of a mutation depends on context and perspective is essential. But what specific mutations drive a cell to become cancerous? Based on current cancer research today, there are 6 defining characteristics that all cancers must have; they can grow on their own, they aren't influenced by anti-growth signals from the body, they invade tissues and metastasize, they replicate endlessly, they trigger angiogenesis, and most importantly avoid apoptosis (Hanahan & Weinberg, 2000). These are known as the hallmarks of cancer and this thesis will mostly focus on apoptosis---a programmed cell death. However, for a cell to become fully cancerous, mutations must qualify each of the hallmarks described above. To understand why, let's think about the context.

Cells in the body are rarely static, they are constantly dividing, changing, and dying. This can serve as a defense mechanism against cancer, as most of the time a cell dies before it has the chance to become cancerous. Ironically, it's in the tissues that this mechanism of cell recycling occurs most frequently that have the highest risk for cancer, i.e. the skin, gut lining, and respiratory tract (Tomasetti & Vogelstein, 2015). The typical life of a cell in these tissues starts from a generic, non-tissue-specific cell called a stem cell. In a living organism, stem cells have the greatest potential to divide, however, they do not divide rapidly (Fuchs 2009). This is because stem cells must protect the human genome, as they are the starting point of cell division and differentiation (Burkhalter et al., 2015). Cell differentiation, in simple terms, is the changing of various cellular characteristics depending on external stimuli from the tissue that the cell is a part of. This is why skin is vastly different from the gut lining in terms of function and physical appearance, yet they started from the same type of stem cell. Cells that have just begun this process of differentiation are similar to a growing child; they divide rather quickly and have the potential to change and acquire many more characteristics that define the type of cell they will be in the future (Weissbein et al., 2014). Once highly differentiated, which is a process that takes time like aging, will eventually lose the capability to divide as they reach the Hayflick limit (Shay & Wright, 2000). The cells that have reached the Hayflick limit in these tissues typically end up in the most exposed regions of the body. Depending on the environment, UV rays blasting the outer skin, or the harsh acidic environment in the gut, these cells eventually die. The 2 main processes that describe cell death are necrosis, a physical disruption of the cell membrane like getting a paper cut, or apoptosis, a programmed cell death when the cell detects internal problems (Hirsch et al., 1997). This process repeats for hundreds of billions of cells in the

average human body every day (Sender & Milo, 2021). This is the reason why cancers do arise. Since the mutations are random, at the end of the day, it's mostly a numbers game.

From the perspective of a cell in the body, its lifetime is relatively short and exists in rather harsh conditions. Not to mention, humans can increase the harsh environments these cells are exposed to by introducing carcinogens such as smoking tobacco and drinking alcohol, both of which lead to an increased risk for cancer (WHO, 2021). Throughout the lifetime of a cell, constant selective pressures are being introduced that will select for mutations to increase its lifetime. Much like the societal pressure of lactose tolerance through an increase in milk consumption. If a highly differentiated cell can't proliferate (cell division), a mutation that overcomes this will be selected. Now a colony of these highly differentiated cells that can proliferate form, and of those, another cell gains a mutation to allow it to proliferate faster. A cell from this new rapidly proliferating colony gains a mutation to avoid apoptosis (programmed cell death). Over many years and mutations, there's now an immortal colony of cells growing and invading surrounding tissues in the body, cancer (Vineis, 2003). The problem is there are a vast number of possibilities in how cancer overcomes each of these hallmarks, which is what makes each cancer unique, and thus hard to diagnose let alone treat.

v. Battles always have casualties

Treating cancer can often be characterized as battling a war at the cellular level, except cancer is an enemy of supercells that require modern-day nukes to defeat. As such, treatments that are effective at battling most cancers result in many casualties of healthy cells and have a heavy toll

on the body in general. Even in cases where cancer is visually obvious, techniques such as surgical intervention can't even remove the entirety of the tumor without the risk of damaging vital organs (National Cancer Institute, 2015).

Breast Cancer:

i. A brief statistic

Breast cancer is the most common among women, and an estimated 2 million new cases were diagnosed as of 2020 (Łukasiewicz et al., 2021). Even with this sex linkage, breast cancer accounts for a majority of cancers diagnosed today. It's estimated that women in the US have a 1 in 8 chance of developing this cancer in their lifetime, and it is the second leading cause of cancer deaths (American Cancer Society, 2024). Let's explore some of the mutations, and contexts that these occur, that make this cancer unique.

ii. Risk Factors

a. Female sex

The context in which mutations occur can also be described as risk factors. Of those, the most notable one is the circulation of hormones such as estrogen. The very reason breast cancer is mainly present in women is that men don't have significant levels of these hormones circulating throughout their bodies. It was observed that higher levels of these hormones, most notably estradiol and estrone, have been linked to an increased risk for breast cancer (Endogenous Hormones and Breast Cancer Collaborative Group, 2013). These hormones are of estrogen origin

and are highest in the absence of menstruation, which can include ovulation, pregnancy, and menopause. There is no specific mutation linked to this phenomenon, but these hormones are observed to increase the proliferation rate of cells that express estrogen receptors (Watson et al., 2008). A receptor is just a protein that promotes a cellular response upon binding to a smaller molecule such as estrogen.

b. Age

Another notable risk factor that doesn't necessarily correspond to any specific mutation is age. Age is a risk factor for most cancers, 75% of which were diagnosed in patients over the age of 55. For breast cancer, it is observed that 80% of patients were over the age of 50 (Benz, 2008). This is mostly due to the cells needing time to acquire mutations that give them an advantage to survive and invade nearby tissues. This observation, alongside proliferation being promoted by estrogen-type hormones, is the primary reason breast cancer is so prominent in women.

c. Family history

This is a risk factor that has been associated with a few prominent mutations, as parents can pass mutations they have down to their children. From a study, 12% of women who had breast cancer reported that they had a first-degree relative with a history of breast cancer (Collaborative Group on Hormonal Factors in Breast Cancer, 2001). Of the mutations that get passed down, those in BRCA1/2 are observed most often (Çelik et al., 2015). These are proteins that initiate homologous DNA repair during the late S and early G_2 phases of the cell cycle. This is called homologous because the repair mechanism requires 2 copies of the cell's DNA, which is after

DNA replication had occurred in the S phase. This repair mechanism uses one copy of the DNA to fill in the gaps of the damaged DNA copy, which is important to reduce the errors that can be made during nonhomologous repair mechanisms (Zhao et al., 2017). In a familial linkage, one parent typically passes on a dysfunctional copy of this BRCA gene, which makes it significantly easier to lose this repair mechanism entirely, as now the cell only has to acquire one additional mutation to lose the only other functional copy of BCRA.

d. General risk factors

Other general risk factors for breast cancer include carcinogens, as the name suggests, they increase the risk for cancer in general and mainly include tobacco and alcohol (Zeinomar et al., 2019). The prolonged use of oral contraceptives as they regulate the estrogen hormone levels in the body. Ethnicity has also been linked to the risk of breast cancer as the highest rates are diagnosed among women of White non-Hispanic ethnic origins (Hill et al., 2019). The highest fatality rates of this cancer include women of a Black ethnicity due to the higher rate of a more aggressive triple-negative breast cancer (TNBC) diagnosis (American Cancer Society, 2024).

iii. Categorizing breast cancer

Breast cancer can be categorized by several factors including the tissue of origin, the stage of prognosis, and the types of hormonal receptors present. More recently, there are classifications of breast cancer based on genomic similarities tied to prognosis and treatment. Triple-negative breast cancer is the focus of this paper, so it would be important to expand on how this cancer is categorized by receptor expression. This approach categorizes breast cancers by expression of

the estrogen receptor (ER), progesterone receptor (PR), and human epidermal growth factor receptor 2 (HER2) (The American Cancer Society medical and editorial content team, 2020). When estrogen derivatives such as estradiol and estrone bind to the ER, the receptor will translocate to the nucleus and serve as a transcription enhancer for cell proliferation genes. In contrast, progesterone modulates the effect of estrogen, as PR inhibits the binding of ER to these enhancer regions (Mohammed et al., 2015). HER2 has a completely different mechanism that is more directly linked to the initiation of the MAPK (Mitogen-Activated Protein Kinase) pathway. Upon binding extracellular mitogens, HER2 can dimerize with another tyrosine kinase receptor to cross-phosphorylate (activate) each other. Once activated, this signals the activation of the MAPK pathway through an adapter protein Grb2 (Sergina & Moasser, 2007). As the name suggests, triple-negative breast cancer (TNBC) has no expression of any of these receptors.

iv. Triple-negative breast cancer

Triple-negative breast cancer accounts for a little more than 10% of all breast cancer cases with a 5-year survival of only 14% in the worst cases (Bauer et al., 2007). The low survival rates are due to the aggressive behavior of the cancer and limited therapeutic options as the cancer lacks targets such as the ER, PR, and HER2 receptors described above. Of the limited targeted therapeutics available, poly(ADP-ribose) polymerase (PARP) inhibitors have proven efficacious in TNBCs that have acquired or stemmed from familial BRCA1/2 deletions (Gonzalez-Angulo et al., 2011). Better characterization of TNBCs can lead to more targeted therapeutic options with lower adverse effects present with general treatments such as chemotherapy due to the low cellular selectivity of this treatment option. One interesting characteristic of this cancer worth exploring is its ability to survive in apoptotic conditions. These cancer cells seem to constantly

be on the verge of apoptosis due to high concentrations of reactive oxygen species (ROS), in other words, oxidative stress (Liu et al., 2023). Better characterization of TNBCs can start with how these cells avoid the programmed death typically associated with high oxidative stress and apoptosis.

v. Zinc in breast cancer

Zinc is the 2nd most abundant trace metal required for all domains of life. Zinc deficiency is a growing global health crisis as an estimated 17% of the world population does not consume adequate levels of dietary zinc, with developing countries in Asia and Africa on the higher end of 24% (Lowe et al., 2024). It is crucial for proper development as it plays important roles in cell proliferation, metastasis, and apoptosis/necrosis. Regarding proliferation, the specific requirement for this trace metal was originally met with conflicting results. A more recent study in the Palmer lab showed depletion of zinc in mammalian cells led to 2 major outcomes, low post-mitotic CDK2 activity (quiescence) and stalled S phase, highlighting the importance of zinc in cell cycle signaling and DNA synthesis/repair (Lo et al., 2020). One meta-analysis of zinc in breast cancers showed there was a correlation between low zinc concentrations in the blood and hair met with elevated zinc concentrations in breast tumors (Jouybari et al., 2019). However, the level of zinc in varying breast cancer subtypes has been met with conflicting results, one study suggested that zinc concentration is higher in ER+ tumors than ER- tumors utilizing X-ray fluorescence microscopy (Farquharson et al., 2009). In contrast, a study that utilized ablation ICP-MS to measure total zinc concluded that TNBCs had the highest levels of zinc (Rusch et al., 2020). These contradicting results are most likely due to the high cellular heterogeneity of a tumor, as a tumor can often be comprised of cancer cells, stroma, extracellular matrix, and even

invading immune cells (Meacham & Morrison, 2013). This tumor heterogeneity can make it difficult to measure levels of zinc in the breast cancer cells alone.

One of the more recent studies in the Palmer lab aimed to address this inconsistency by measuring cytosolic labile zinc in various cancer cell lines to determine zinc homeostasis and the importance of zinc in cell viability and proliferation (Woyciehowsky et al., 2025). This research concluded results similar to the study utilizing ablation ICP-MS, in that TNBCs generally contained the most zinc compared to other breast cancer subtypes showcased by relatively high concentrations of labile (free) zinc in MDA-MB-231 and MDA-MB-157 cell lines compared to non-transformed MCF10A epithelial breast cells; with luminal A breast cancer subtypes containing the least showcased by relatively lower concentrations of labile zinc in T47D cells. What stands out from this experiment is the TNBC's characteristic to resist a change in cytosolic zinc when grown in increasing extracellular zinc conditions. In general, mammalian epithelial breast cells, cancerous or not, show an increase in proliferation when grown in higher levels of extracellular zinc (up to 30 μM $ZnCl_2$). When increasing concentrations of extracellular zinc further (>100 μM $ZnCl_2$), cell proliferation became more dependent on subtype, with TNBCs showing the highest proliferation in the most extreme case of 500 μM $ZnCl_2$, Not only do these TNBC cells proliferate the most in these high Zn conditions, but their resilience to high levels of extracellular zinc seems to be a notable characteristic compared to other breast cancer subtypes. However, this resilient characteristic is not observed in low concentrations of extracellular zinc, and in general, mammalian epithelial breast cells show decreased proliferative activity, the breast cancers of the lowest activity compared to a healthy non-transformed cell line MCF10A. The problem with measuring the proliferative activity alone is that it does not provide information on

cell viability, i.e. whether the cells are dying due to a shortage of zinc or entering a state of quiescence.

Apoptosis:

i. Pathway overview

Apoptosis, a term originating in the early 70s, is a form of irreversible, programmed, cell death, complimentary to mitosis associated with cell proliferation (Kerr et al., 1972). This pathway is distinct from necrosis which is a cell death associated with an external disturbance of the cellular membrane (Hirsch et al., 1997). That being said, apoptosis occurs due to internal factors such as DNA damage from overexposure to UV radiation or high oxidative stress from ROS (Norbury & Hickson, 2001). The main regulator of this pathway is the protein P53, which in the presence of DNA damage, activates a cascade of pro-apoptotic factors leading to the death of a problematic cell (Williams & Schumacher, 2016). This pathway is a vital defense mechanism against cancer formation in the body and makes it crucial to understand how cancers defend against this process.

ii. Apoptotic defense in TNBCs

Most cancers, aside from malignant melanomas, avoid apoptosis by inheriting a mutated copy of P53 (Mendiratta et al., 2021). For proper function, this protein has to form a homodimer with itself and any incorporation of a mutated form of the protein into this homodimer results in a nonfunctional protein complex (Wong, 2011). This is then especially prominent in cancers as

only one of the TP53 alleles needs to acquire a mutation to lose more than 90% of this pathway's overall function. Another notable defense mechanism is an elevation of anti-apoptotic proteins of the Bcl-2 family (Bcl-xL, Mcl-1, and Bcl-2), which inhibit a pro-apoptotic factor, Bax. The relative ratio of Bax:Bcl-2 in a cell determines whether that cell will undergo apoptosis, and TNBCs have been shown to have elevated expression of these Bcl-2 proteins as their main defense mechanism. This is such a strong defense mechanism that these cells are even shown to be resilient to chemotherapy (Nocquet et al., 2024), a treatment that strongly promotes apoptosis during mitosis by interfering with spindle formation, a fundamental step for proper chromosome inheritance to the daughter cells upon division.

iii. Zinc in Apoptosis

There are many reasons why apoptosis is worth exploring with respect to cell viability in response to changes in extracellular zinc. The main reason is that zinc directly interacts with the apoptosis pathway through various apoptotic factors such as P53, P21, and caspase 3 (Fanzo et al., 2002). This paper concluded that an increase or decrease in extracellular zinc resulted in an increase in P53 and P21 mRNA levels, and caspase 3 activity was shown to decrease in high extracellular zinc conditions. This correlation to zinc with regards to apoptosis is important to research in breast cancers such as TNBC as it can provide more information about the ways these cancers not only defend against apoptosis but also how future therapeutics may be able to take advantage of where these cells lack in apoptotic defense. This thesis aims to answer two main questions: When TNBC cell lines are grown in varying extracellular zinc conditions, specifically low zinc extracellular zinc conditions, is this low proliferative observation due to entering a state of quiescence, or are the cells dying? [AND] If the cells are dying, along with the observed effect

of zinc inhibiting cas3 and activating transcription of P53/P21, does low extracellular zinc promote apoptosis in these TNBC cells?

---------- **Methods** ----------

Media Recipes:

i. MCF10A:

- Full Growth Media (FGM): DMEM/F12 media + 5% fetal bovine serum (FBS) + 1% penicillin/streptomycin (pen/strep) antibiotics + 20 ng/mL EGF + 0.5 mg/ml hydrocortisone + 100 ng/ml cholera toxin + 10 mg/ml insulin.
- Minimal Media (MM): 50:50 Ham's F12 phenol red free/FluoroBrite™ DMEM + 1.5% Chelex® 100-treated FBS + 1% pen/strep antibiotics + 20 ng/mL EGF + 0.5 mg/ml hydrocortisone + 100 ng/ml cholera toxin + 10 mg/ml Chelex® 100-treated insulin.

ii. MDA-MB-231 & MDA-MB-157:

- FGM: Leibovitz's L-15 Medium (catalog no 30-2008) + 10% FBS + 1% pen/strep antibiotics
- MM: Leibovitz's L-15 Medium (catalog no 30-2008) + 1.5% Chelex® 100-treated FBS + 1% pen/strep antibiotics

Cell Culture:

i. Rationale

Cell culture is a method used to grow cells *in vitro* to have a population of cells to perform experiments on. Cells divide at different rates depending on the cell line and growth media. The cell lines used in these experiments were MCF10A, MDA-MB-231, and MDA-MB-157. Growth media can be characterized into 2 main categories: full growth media (FGM) and minimal growth media (MM). Cell culture is performed inside a BSL-2 biosafety cabinet to eliminate

outside pathogens from contaminating the cell lines. Everything that enters the hood gets sprayed down with 70% ethanol to increase this level of decontamination further.

ii. Starting a colony

Since MCF10A, MDA-MB-231, and MDA-MB-157 cells are adherent, cells were cultured in adherent dishes/flasks. To start a fresh cell culture, frozen cell stocks (stored in liquid N_2) were rapidly thawed in a 37°C water bath. Before thawing the cells, the FGM solution was warmed at 37°C water bath for 20-30 min. Thawed cells were then directly pipetted into a pre-warmed FGM solution and transferred to the cell culture dishes or flasks. The volume of FGM added to the flasks depends on the surface area of the dish/flask as there needs to be enough mitogens/nutrients present for the cells to grow, but also a small enough volume that the cells acquire O_2 and CO_2 through the surface aeration (mixing of gas and liquid molecules). For example, 12 mL FGM was added in a T-75 flask whereas 25 mL FGM solution was used for T-125 flasks. After transferring cells into flasks, they were labeled with the cell type, date, and the passage number (with a completely new cell line this would be passage Cells were mostly grown in two sizes of flasks for different experiments: T-75 flasks with a surface area of 75 cm^2 for the live/dead assay and T-125 flasks with a surface area of 125 cm^2 for the apoptosis assay. MCF10A cells were kept at 37°C, 90% humidity, and 5% CO_2 incubator whereas MDA-MB-231/157 cells were grown in an incubator at 37°C, 90% humidity, and 0% CO_2.

iii. Passaging a colony

Passaging cells is essential to reduce the amount of unnecessary cell-to-cell contact and serve to replace the old FGM the cells have been growing in with fresh media. To passage these cells, aspirate out the old media from the flask containing the cells. Old media can also contain cells that have just actively divided (cells suspend off during division before adhering back down onto the dish) and dead cells (a cell is considered dead if it has a compromised membrane). After all the old media is aspirated out, wash the cells 2-3 times with 5 mL (use 7mL when passaging cells in a T-125) of Dulbecco's Phosphate Buffered Saline (DBPS). Then, pipette 5 mL (once again 7 mL for a T-125) of 0.05% Trypsin + EDTA into the flask of MCF10A cells and 0.25% Trypsin + EDTA into the flask of MDA-MB-231 cells. Place the cells back into their respective incubators for 15-30 min. The amount of time can depend on several factors: the number of cells in the flask (confluency), the cell line, and the strength of the trypsin. In this case, a fully confluent flask of MCF10A cells, being trypsinized at 0.05% takes at most 30 min, and a fully confluent flask of MDA-MB-231, being trypsinized at 0.25% takes at most 20 min. *Note: at the 15-minute mark it can be useful to view the cells under a microscope every 5 min to see how far along the trypsinizing process is.* Once the cells have been completely suspended off the dish, quench the trypsin reaction by adding a 1:1 ratio of FGM. Then, transfer the suspended cells into a centrifuge tube and centrifuge the cells at 1000rpm for 5min.

While the cells are centrifuging, pipette 12 mL of warmed FGM into a new T-75 flask. Label, the new flask with the cell type, date, and new passage number which increases after each passage. When the centrifuge process is over, there will be a small pellet of cells at the bottom of the centrifuge tube. Depending on the number of cells present before centrifuging, it can either be

easily visible or relatively hard to see. Regardless, it can be fairly easy to dislodge this pellet so handle it with care. Once the pellet is obtained, aspirate out the trypsin-media solution from the tube, once again with care as the pellet can also get aspirated out (leaving a small amount of residual solution can avoid this). Then, resuspend the pellet in 1 mL of warmed FGM. To ensure the cells are homogenously suspended, use the same pipette to moderately pipette up and down to break up the pellet completely (there should be no visible signs of the pellet floating). Pipette 250ul of this now homogenous solution of cells into the newly labeled T-75 flask. *Note: This is a 1:4 passage optimized to grow these cells back to confluency in 2-3 days.* Place the cells back into an appropriate incubator (MCF10A: 90% humidity, 37°C, and 5% CO_2---MDA-MB-231: humidified, 37°C, and 0% CO_2).

Live/dead assay:

i. Rationale

Previous work in the Palmer lab provided evidence that altering the levels of extracellular zinc changed the level of cellular activity across multiple breast cancer cell lines compared to a non-cancerous cell line, MCF10A, by measuring mitochondrial activity in a cell. However, mitochondrial activity alone failed to distinguish a cell that has entered a state of senescence/quiescence (low mitochondrial activity) from a dead cell whose mitochondrial activity is no longer measurable. MCF10A and MDA-MB-231 cells when introduced to zinc deficiency (ZD) by incubating cells with a Zn^{2+} chelator, tris(2-pyridylmethyl)amine (TPA) showed lesser proliferation. From our previous live/dead assay on MCF10A cells, we knew that these cells were not dying but they were entering a state of quiescence. MCF10A cells also showed lower levels of

proliferation in the presence of high extracellular zinc with $ZnCl_2$. In contrast, the MDA-MB-231 cells showed no change in proliferation in high zinc. Additionally, live/dead assay on MCF10A cells confirmed that the cells were dying in high Zn. However, we were unsure about the fate of MDA-MB-231 cells in low zinc. Hence, the goal of the live/dead assay on MDA-MB-231 cells was to first fill in the gaps of missing data and then obtain a full understanding of whether MDA-MB-231 cells were becoming quiescent or senescent or dying at low extracellular zinc.

ii. Live/dead assay mechanism and data collection

The assay utilizes a ReadyProbes™ Cell Viability Imaging Kit manufactured by Invitrogen™ containing two probes: Nucblue™ Live reagent (Hoechst) and Nucgreen™ Dead reagent (SYTOX green). Hoechst is membrane permeable and stains the nucleus of every cell to give a total cell count with a maximum excitation/emission of 360/460 nm. SYTOX green is not membrane permeable, therefore, it will only stain the nucleus of cells that have compromised membranes which are considered a dead cell with a maximum excitation/emission of 504/523 nm. The number of dead cells divided by the total number of cells equals the fraction of dead cells. A Nikon HCA microscope equipped with an LU-NV Laser unit supporting up to eight laser wavelengths and an LED light source was used for imaging of the probes. Hoechst gets excited by the 405 nm laser and the emission is captured in the DAPI filter ranging from 435 – 480 nm at 75% power, with a 5 s exposure time. SYTOX green gets excited by the 488 nm laser and the emission is captured in the GFP filter ranging from 500 – 550 nm at 15% power, with a 50 ms exposure time. The power percentage and exposure time were optimized prior to running this assay with the MDA-MB-231 cell line. The cells were grown in a 96-well plate with 16 wells dedicated to each extracellular zinc condition. Images were taken from 3 different fields of view

of each well, producing a total of 48 images for each condition in one run of the assay. A MATLAB pipeline created by a former lab member was used to interpret the images from the microscope. By determining a cell nucleus from the DAPI channel, it counted the total number of nuclei in the image (total cell count), and then it counted the total nuclei from the GFP channel (total dead cell count). Each point on the final graph represents a single image vs. the fraction of dead cells present in that image, and images were separated into their corresponding extracellular zinc condition.

iii. Optimizing the live/dead assay protocol for MDA-MB-231(157) cells

This protocol had been fairly optimized in the lab, but there were still gaps in these data that had been in the works before starting the live/dead assay. The MDA-MB-231 cell line already had a biological replicate of data collected, so the first couple of assays would be for this cell line while an MDA-MB-157 cell line was thawing. When first working with the MDA-MB-231s and MDA-MB-157, they often look more confluent than they are compared to the MCF10A cell line, as the MDA-MB-231 cells spread out and occupy more space. As a result, the main challenge was having enough of the cells present to begin an experiment, especially with the MDA-MB-157s as they not only take up more space like the 231s but also grow around 3 times slower.

The first experiment with the MDA-MB-231 started by making up a 14 mL solution of 350,000 cells as the goal was to plate 5,000 cells in 64 wells of a 96-well plate with each well containing 200 µL of solution. This would require 12.8 mL of a 25,000 cell/mL solution, and the 14 mL solution was made to ensure there was more than enough to meet this goal. An 8-channel pipette

was used for the duration of these experiments and in this first experiment, the cells were plated row by row from top to bottom. Towards the end of the plating, the basin that had comprised the solution of cells started to run low and the H4 well didn't get an equivalent amount compared to the rest. The cells were then transferred into a humidified, 37°C incubator with 0% CO_2 for 24 hours.

While the cells were incubating, a series of MM solutions were made with varying concentrations of zinc and one with a zinc chelator TPA. The first solution made was 10 mL of the 2ZD (zinc deficient) solution for which 2 µL of 0.01 M TPA was added into 10 mL of MM. Then, the two zinc-rich solutions were made by adding 3 µL of 0.1 M $ZnCl_2$ into 10 mL of MM (30ZR) and 15 µL of 0.1 M $ZnCl_2$ into 10 mL of MM. The three defined zinc media in 14mL centrifuge tubes were then stored in a refrigerator. Since it requires 3.6 mL of the media to replace 16 wells with 200 µL solution, this would be enough media to run at most two assays.

Once the first incubation period was finished, a multichannel pipette was used to aspirate out the FGM from the wells that the cells were initially plated in and were replaced with the defined zinc media prepared. This was done by completely aspirating out every well first, and then row by row, 200 µL of 2ZD to rows A and B, 200 µL MM to rows C and D, 200 µL 30ZR to rows E and F, and 200 µL 150ZR to rows G and H was added to a total of 64 rows of a well plate. The final plating resembled **Table 1** below and then the cells were placed back into the same incubator for

an additional 48 hours before prepping them for imaging.

96-Well	1	2	3	4	5	6	7	8
A	2 μM TPA MM	2 μM TPA MM	2 μM TPA MM	2 μM TPA MM	2 μM TPA MM	2 μM TPA MM	2 μM TPA MM	2 μM TPA MM
B	2 μM TPA MM	2 μM TPA MM	2 μM TPA MM	2 μM TPA MM	2 μM TPA MM	2 μM TPA MM	2 μM TPA MM	2 μM TPA MM
C	MM	MM	MM	MM	MM	MM	MM	MM
D	MM	MM	MM	MM	MM	MM	MM	MM
E	30 μM ZnCl2 MM	30 μM ZnCl2 MM	30 μM ZnCl2 MM	30 μM ZnCl2 MM	30 μM ZnCl2 MM	30 μM ZnCl2 MM	30 μM ZnCl2 MM	30 μM ZnCl2 MM
F	30 μM ZnCl2 MM	30 μM ZnCl2 MM	30 μM ZnCl2 MM	30 μM ZnCl2 MM	30 μM ZnCl2 MM	30 μM ZnCl2 MM	30 μM ZnCl2 MM	30 μM ZnCl2 MM
G	150 μM ZnCl2 MM	150 μM ZnCl2 MM	150 μM ZnCl2 MM	150 μM ZnCl2 MM	150 μM ZnCl2 MM	150 μM ZnCl2 MM	150 μM ZnCl2 MM	150 μM ZnCl2 MM
H	150 μM ZnCl2 MM	150 μM ZnCl2 MM	150 μM ZnCl2 MM	150 μM ZnCl2 MM	150 μM ZnCl2 MM	150 μM ZnCl2 MM	150 μM ZnCl2 MM	150 μM ZnCl2 MM

Table 1: This table represents the layout of the 96-well plate for which the cell line was incubated for 48 hours before imaging preparation.

Right before the end of the 48-hour incubation period, an1800 μL mixture was prepared that had a 1:1 ratio of Nucblue™ and Nucgreen™ dye solutions used for imaging. Then, the cells were removed from the incubator and 100 μL of media was aspirated out from each of the wells. 28 μL of the dye mixture was then added to every well and the cells incubated in the dye for an additional 20 minutes. During this final incubation period, the parameters for imaging were set on the Nikon HCA (DAPI: 75% power and a 5 s exposure, GFP: 15% power and a 50 ms exposure all on a 20x objective). The cells were now ready to be imaged, and a pipeline made by a former lab member was used to take images of every well at a given field of view (FOV) following the DAPI and GFP parameters. The pipeline was run 3 different times with 3 different FOVs to produce at most 48 technical replicates for each media condition the cells were grown in. Once all the images were taken, they were run through another pipeline in MATLAB. This

protocol automatically segmented individual nuclei in a FOV and then counted the total nuclei in each channel. This gave total cell counts from the Hoechst-stained nuclei, and then the dead cell counts from the SYTOX green-stained nuclei from each image. The fraction of dead cells in each technical replicated was then plotted on a graph of the defined zinc media condition vs. the fraction of dead cells.

From this assay, there were a few things we noted for the subsequent assays performed. The initial 14 mL solution of cells ran out before the cells were completely plated, so 15 mL solutions were made up from then on. Another trend we noticed was the cell counts tended to drop from the topmost row to the bottommost row of the plate, which was an issue as the cells were treated in the various zinc conditions row by row. To account for this, the cells were platted column by column for the duration of the experiments, so that there were more consistent cell counts throughout the conditions they were treated in. The biggest issue with this first experiment was the MDA-MB-231 cells spreading out in the well similarly to how they spread out in the flask before starting the assay, which led to drastically smaller cell counts compared to the MCF10A cells that didn't take up as much physical space. The initial idea was to plate more cells during the initial plating of the experiment, but that could have led to more complex changes in how the cells interact with the various zinc conditions, so instead, the 20x objective was changed to a 10x objective to collect a wider FOV and hence image more cells. To account for this change when processing the images with the pipeline in MATLAB, the code used to determine a nucleus where the dye would be expressed was given smaller bounds to avoid unwanted clumping of multiple nuclei as one count. We decided taking notes during the imaging process of wells would be efficient to exclude any technical replicates from the final results that had weird dye

interactions (seen with overexposure in either DAPI or GFP channels) or drastically small cell counts in a given FOV as it reduces the statistical significance compared to wells that have more of the cells in the image.

After making the necessary changes for imaging the MDA-MB-231 cells, the rest of the assays ran smoothly, and each subsequent biological replicate photocopied the last. The MDA-MB-157 cell line was remarkably similar in appearance, and they spread out on a plate like the MDA-MB-231s, so the changes to imaging for the MDA-MB-231 cell line translated over to the imaging for the MDA-MB-157 cell line. The only major difference is the MDA-MB-157 cell line grows approximately 3 times slower, so the only major change was passaging more of the cells at a less frequent rate to meet the 375,000-cell demand for the assay itself.

iv. Live/dead assay protocol on MDA-MB-231(157) cells

Using MDA-MB-231 FGM, dilute a cell pellet collected during a passage to 25,000 cells per mL and keep 15 mL of this solution for the initial 96-well plating. Pipette 200 µL of this solution into an 8x8 grid column by column on a 96-well plate. The goal is to plate roughly 5000 cells per well. After plating, incubate the cells at 37°C and in 0% CO_2 for 24 hours. During this incubation period, prepare the extracellular zinc media conditions which include: 2ZD (2 µM TPA in MM), 30ZR (30 µM $ZnCl_2$ in MM), 150ZR (150 µM $ZnCl_2$ in MM), and a control solution of unaltered MM. Preparing 10 mL of each of these solutions allows up to 2 assay runs and they can be stored just like MM. After 24 hours have passed, using a pipette, carefully aspirate the FGM out from the wells. *Note: tilting the plate and pipetting from the edge of the well reduces the risk of*

aspirating out adherent cells. Next, pipette 200uL of each defined zinc media solution into 2 rows of the 8x8 grid. After replacing the media, there should be a total of 16 wells per zinc condition, including the MM control. Place the well plate back into the incubator for an additional 48 hours. Within the last 30 minutes of this incubation period, prepare a 1:1 solution of SYTOX green and SYTOX blue reaching a final volume of 1800 µL. After the incubation period, aspirate out 100 µL of media from every well with a pipette and then add 28 µL of the SYTOX dye mixture to the remaining 100 µL of each well. Return the cells to an incubator for an additional 20-30 min to allow the dyes to bind. During this time, set up the microscope to collect the images of the wells. The pipeline for this experiment used a 10x objective and acquired images of the center, left side, and top side of each well with DAPI (75% at 5s exposure) and GFP (15% at 50ms exposure) to excite the corresponding dyes. The microscope didn't acquire the 3 perspectives in a single pipeline, rather, the center images were collected first, then the left side, and finally the top side, producing 64 images per pipeline and 192 images in total.

Apoptosis assay:

i. Rationale

After discovering MDA-MB-231 cells were dying in low extracellular zinc conditions from the live/dead assay, we got motivated to explore the mode of death of MDA-MB-231 cells, i.e. apoptosis or necrosis. Since low zinc can initiate transcription of p53 and p21 and no longer has an inhibitory effect on Caspase3 in contrast to high zinc, we hypothesized that apoptosis might be getting induced in these cells. MCF10A cells can serve as a control as they are non-transformed healthy epithelial breast cells, and they appear to die in high extracellular zinc conditions, unlike the MDA-MB-231 cell line.

ii. Assay mechanism and data collection

The Annexin V assay was first proposed by Koopman in 1994, after the discovery of a protein, Annexin V, that binds to inner membrane phospholipids, which become present on the outside of the cell during apoptosis through a membrane inversion (Koopman et al., 1994). This assay utilizes two probes; Alexa Fluor™ 647 annexin conjugate and Nucgreen™ SYTOX green nuclear stain, both manufactured by Invitrogen™. The first probe is Alexa 647 which conjugates to Annexin V that binds to phosphatidylserine present on early and late apoptotic cells. The second probe is SYTOX green which stains the nuclei of cells with compromised membranes (dead) by sliding between the base pairs on strands of DNA. Alexa 647 and SYTOX green are not membrane permeable, and thus cannot bind to either target of a healthy non-apoptotic cell. Early apoptosis is quantified by the binding of Alexa 647 alone, as the membrane is still mostly intact. Late apoptosis is quantified by binding of both Alexa and SYTOX, as the membrane is

mostly disrupted, and binding of SYTOX alone would suggest early necrosis as the membrane is slightly compromised with no inversion. The intensities of the fluorophores are measured on a BD Accuri™ C6 Plus flow cytometer that has 2 lasers and 4 filters (a 488nm laser with filters: 533/30. 585/40, and 670/LP, and a 640nm laser with a 675/25 filter). SYTOX green is excited by the 488nm laser and measured with the 533/30 filter, and Alexa 647 is excited by the 640nm laser and measured with the 675/25 filter. There is a relatively high cell count for this experiment when working with the cytometer, so the sorting process must be slow to avoid clumping of cells and a 2-micron filter is used beforehand to avoid cell clumping as well. During the collection process, 5 plots are made to analyze the data later with the Accuri analysis software. The plots include: FSC (forward scatter) vs. SSC (side scatter), FSC height vs. FSC area, Alexa 647 vs. SYTOX green, Alexa 647 histogram, and SYTOX green histogram. There are 2 gates made to filter out non-cellular particles and possible doublets of cells. On the Alexa 647 vs. SYTOX green plot, a cross-section is placed to create 4 quadrants: lower left = healthy cells, lower right = early apoptotic cells, upper right = late apoptotic cells and necrotic cells, upper left = necrotic cells and small cell fragments. The Accuri analysis software provides percentages for each of these quadrants.

iii. Optimizing the apoptosis assay protocol

Before running any apoptosis assays, 150 mL of the annexin-binding buffer was made as it can be stored at room temperature for the duration of the project. The solution is composed of 10 mM HEPES, 140 mM NaCl, and 2.5 mM $CaCl_2$ diluted in Milli-Q water at a pH of 7.4 ± 0.05. After preparing the buffer solution, the first assay was performed on the MCF10A cell line since it would serve as a control cell line, time was needed to start up a new colony of MDA-MB-231

cells after the end of the live/dead assays. For the first assay, we planned to run the experiment with a 3ZD (3 μM TPA) and 150ZR (150 μM ZnCl2) condition to determine the effects of zinc at the two extremes from the live/dead assay alongside a positive control (6 μM doxorubicin 14hr), a negative control (unaltered MM), and untreated cells for the gating process on the cytometer. Initially, 1 million cells were plated in 5 wells of a 6-well plate in 2 mL of MM. After 24 hours, the MM was aspirated out of the two condition wells (3ZD and 150ZR) and was replaced with prepared 3ZD and 150ZR solutions. The cells were then incubated for an additional 24 hours and 14 hours before harvesting the cells, 6 μM doxorubicin was added to the positive control well.

When harvesting the cells, the supernatant of each well was collected in separate 10 mL centrifuge tubes to keep any apoptotic cells that may have lifted off the plate. Each well was washed 2 times with cold D-PBS and then trypsinized with 1 mL of warm 0.05% trypsin + EDTA for 15 min. Once the cells lifted off the plate, the trypsin was neutralized with the media conditions the cells were initially treated in and they were then transferred into their respective centrifuge tubes that contained the supernat that was collected before trypsinizing. At this point in the experiment, there were five 14 mL centrifuge tubes (3ZD, 150ZR, positive, negative, and untreated). The cells were then centrifuged down to a pellet, the supernatant was then aspirated out and the pellet was resuspended in 500 μL of the annexin-binding buffer. There was an attempt to count the cells in each condition, however, the dye used to count the cells was binding to the cells strangely in the annexin-binding buffer and an accurate cell count was not obtained, so instead, all the resuspended cells were transferred into 3 mL centrifuge tubes and were centrifuged down to a pellet once again. During this centrifuge, the annexin-binding dye

solutions were prepared by adding 5 µL of the annexin conjugate acid solution and a drop (~17 µL) of SYTOX green into 488 µL of the annexin-binding buffer. Once the cells finished centrifuging, all the condition and control pellets were resuspended in 100 µL of the annexin-binding dye mixture (except the untreated control) to leave in the dark for 20 minutes to allow the fluorophores to bind. The untreated control was resuspended in 500 µL of the annexin-binding buffer without the dyes and was ready for analysis. After 20 minutes, all the volumes of the tubes were brought to 500 µL with an additional annexin-binding buffer, and transferred each condition/control into cytometer tubes utilizing a 50-micron filter to separate any conjugated cells. All the conditions/controls were then ready to be analyzed on the cytometer.

From this first assay, we learned how to use the BD Accuri C6 plus which is the cytometer that the apoptosis assay would be carried out on. In addition to the timing of the assay which was helpful with planning out experiments.

The next couple of assays were performed on the MDA-MB-231 cell line, for which 500,000 cells were initially plated due to a shortage of cells available for the assay. The parameters for these assays were treating the cells in a 3ZD and 150ZR condition for 24 hours. The timing for adding the positive control which was 6 µM Doxorubicin did not align well with the timeframe for harvesting the cells, and in these assays, the doxorubicin was not added with enough time to induce apoptosis in the cells. Single fluorophore controls were added in unaltered MM conditions to test unwanted dye interactions, and the amount of fluorophore used in this

experiment was 1:100 Alexa 647 and 2:100 SYTOX green. The cells were treated with the fluorophores for 20-25 minutes before they were analyzed on the cytometer.

These two assays were still much of a learning process for the assay itself. The main takeaways from these assays were finding a different positive control that worked better with the timing of the harvesting processes (3-4 hours), growing the cells in a larger flask to have closer to $1x10^6$ cells to plate, and counting the cells during the harvesting process was still problematic. Moving forward, a new apoptotic inducing agent was used for the positive control, camptothecin, added 24 hours before harvesting the cells, the MDA-MB-231 cells were grown in a T-125 flask which can grow about twice the amount of cells than the T-75, and counting the cells during the harvesting process of the protocol was removed so only an initial plating density will be measured.

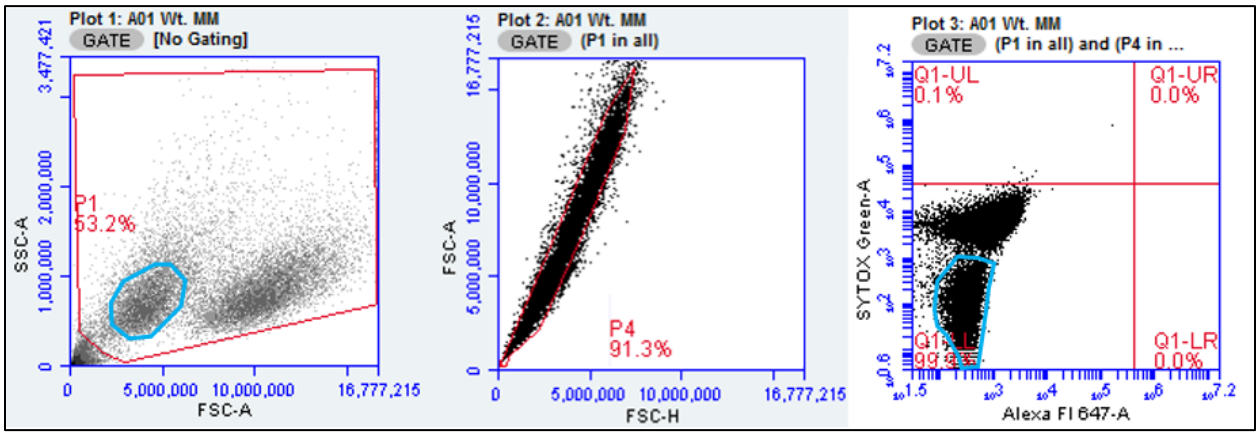

Figure A: This figure shows 2D plots of the forward scatter area (FSC-A) vs. side scatter area (SSC-A) on the left, the forward scatter height (FSC-H) vs. FSC-A in the middle, and Alexa 647 vs. SYTOX green on the right. P1 and P4 represent the gates used to filter the collected data. The

blue outline in the left and right plots shows an abnormal doublet population of cells that appeared in this assay.

This next assay identified an issue that occurred a few times during the duration of acquiring data for these experiments. The issue is the appearance of a second population of cells that were not present in previous assay runs and affects every condition and control in the biological replicate. **Figure A** above shows the gating of the untreated control where the second population is traced in blue and is only identifiable in the FSC-A vs. SSC-A plot and the 2D plot of the fluorophores. The major issue with this second population is that it appears where the possible apoptotic cells would appear in the FSC-A vs. SSC-A graph, so the P1 cannot exclude these cells from the data. As of now, the results from any assay that this phenomenon occurred can't be interpreted because the origin of this population is unclear.

The next assay run on MDA-MB-231 cells had an incubation period of 24 hours for the 3ZD and 150ZR conditions. The positive control used in this assay was 18 μM camptothecin with a 24-hour incubation period. A lab member had optimized camptothecin-inducing apoptosis in MCF10A cells at 6 μM for 24 hours, which was better timing for the assay compared to the 14 hours doxorubicin needed to be added. Mistakenly, the protocol was followed using the stock concentration of doxorubicin which was 2 mM in comparison to the 6 mM stock concentration of camptothecin. This error resulted in a final concentration of 18 μM camptothecin instead of the planned 6 μM camptothecin. The assay was performed using a 12-well plate and it has roughly half the surface area of the 6-well plate, so 500,000 cells were plated in 1 mL of MM to

account for the decrease in surface area of the well. Using the 12-well plate was to account for the single Alexa 647 and SYTOX green controls since it required a total of 7 wells to perform the assay which would have had a high demand of 7 million cells if a 6-well plate was used. Nearing the end of the harvesting process, the conditions/controls were incubated in 1:100 Annexin V-Alexa 647 and 2:100 SYTOX green for 20 minutes. This assay did not run into the second population problem and no other issues arose during the protocol of the assay itself.

From this assay, we learned that the 18 μM camptothecin may be a more fitting concentration than 6 μM, given that the MDA-MB-231 cells appeared to be highly resistant to apoptosis compared to the MCF10A cell line. The 12-well plate worked well with the single controls that originally demanded a high cell count that was never met using two 6-well plates, however, at this point two biological replicates of the single controls were collected that appeared to phenocopy, so the single controls were no longer necessary to include in future assays.

The next assay was performed on the MDA-MB-231 cell line with an incubation period of 48 hours in the 3ZD and 150ZR conditions. Since the goal of these first few assays on the MDA-MB-231 cells was to catch apoptosis early (if it's occurring), we were curious to see the behavior of the cells when incubating them for longer periods, similar to the incubation period of the live/dead assay. The negative control was unaltered MM, and the positive control was 18 μM camptothecin for 48 hours. Initially, we had regretted changing two variables at the same time (incubation period and positive control incubation period), but camptothecin was not necessarily

optimized for the MDA-MB-231 cells at this point either way nor was the timing of apoptosis in this cell line if it had been induced in the 3ZD condition.

The final two assays were performed on the MCF10A cell line with an incubation period of 24 and 48 hours to compare to the results collected from the MDA-MB-231 cell line. The major change to this assay was the incubation period of the probes, which only incubated for 15 min before imaging. The goal of this was to avoid unwanted interactions between these probes that could occur in longer incubation periods.

iv. Final protocol

Prepare the annexin-binding buffer reagent beforehand, it can be stored in a sealed glass beaker at room temperature for the duration of the experiment. The annexin-binding buffer is 10 mM HEPES, 140 mM NaCl, and 2.5 mM $CaCl_2$ diluted in 150 mL Milli-Q H_2O at a pH 7.4 +/- 0.05.

After collecting a cell pellet during a passage, dilute this pellet in the respective cell line's MM to 500,000 cells/mL and add $1x10^6$ cells (2 mL solution) to 5 wells of a 6-well plate. Label the wells accordingly: untreated control, MM (negative) control, camptothecin (positive) control (MDA-MB-231 positive control → 18 µM camptothecin | MCF10A positive control → 6 µM camptothecin), 3 µM TPA (3ZD), and 150 µM $ZnCl_2$ (150ZR). Then, incubate the cells for 24 hours (MDA-MB-231 → humidified, 37°C, 0% CO_2 | MCF10A → humidified, 37°C, 5% CO_2). During this incubation period, prepare the extracellular zinc solutions (3ZD: 3 µM TPA in MM, 150ZR: 150 µM $ZnCl_2$ in MM). After this incubation period, replace the media of the wells; for

the controls, replace the MM with fresh MM, and for the conditions (3ZD and 150ZR), replace the media with their respective zinc conditions prepared during the incubation period. The volume in the plates should remain the same as the initial plating volume of 2 mL. If incubating for 24 hours, add the camptothecin in the positive control well (MDA-MB-231: 18 μM camptothecin, MCF10A: 6 μM camptothecin), and if incubating the cells for 48 hours, add the camptothecin after an initial 24 hours at the same concentration for the 24-hour incubation experiment. *Note: camptothecin is a DNA-damaging reagent that induces apoptosis and the incubation period for this to occur is 24 hours before harvesting the cells for the cytometer.*

Right before the end of the final incubation period label 5 x 14 mL centrifuge tube, 5 x 1 mL centrifuge tubes, and 5 cytometer tubes with the same labels for the controls and conditions labeled on the 6-well plate. Put the DPBS and annexin-binding buffer into an ice bath and place the MM and MM conditions into a 37°C water bath 30 minutes before harvesting the cells. *Note: during the collection process, every control and condition must remain separate from one another as each will be analyzed separately on the cytometer.* After the final incubation, collect the supernatant of each well into the 14 mL cytometer tubes, wash each well with cold DPBS at least 3 times, and then trypsinized every well (MDA-MB-231 → 1 mL 0.25% trypsin + EDTA 10-15min, MCF10A → 1 mL 0.05% trypsin + EDTA 20-30min). After the trypsinizing reaction, neutralize the remaining trypsin with 1 mL MM in the control wells, 3 μM TPA MM in the 3ZD well, and 150 μM $ZnCl_2$ in the 150ZR well. Collect the resuspended cells in their respective 14 mL centrifuge tube. Centrifuge the cells at 1000 rpm for 5 min. After the centrifuge process, carefully aspirate out the supernatant from each tube. *Note: the pellets will be quite small, especially when working with a 12-well plate, so keep the aspirator pipette tip far from the pellet*

at the bottom of the tube. Leaning the tube and letting the supernatant fall into the aspirator pipette has proven effective. Resuspend each cell pellet in 500 µL of cold annexin-binding buffer and transfer the resuspended cells into their corresponding 1 mL centrifuge tube. Centrifuge the resuspended cells again at 1000 rpm for 5 min.

During this centrifuge process, prepare the fluorophore solutions. Start by adding 5 µL Alexa 647 acid conjugate into 485 µL of the annexin-binding buffer, then add 10 µL of SYTOX green to this solution; store in the dark until cells are done centrifuging. After collecting the cells from the centrifuge, using a pipette, carefully pipette out the supernatant. *Note: the cell pellet will be nearly invisible, so orientating the tubes in the centrifuge to know where the pellet will form is helpful.* For the untreated control, resuspend the pellet in 500 µL annexin-binding buffer, and then resuspend the negative, positive, 3ZD, and 150ZR pellets in 100 µL of the annexin-binding buffer containing both SYTOX green and Alexa 647. Leave the cells in the dark for no longer than 20 min to allow the fluorophores to bind. Afterward, add 400 µL annexin-binding buffer to each tube except the untreated control, and using a 2-micron filter, filter the cells into the corresponding centrifuge tubes. Place these tubes in an ice bath and start the centrifuge process quickly thereafter.

---------- **Results & Analysis**----------

Live/dead assay:

Prior research carried out in the lab discovered a significantly lower degree of metabolic activity for the triple-negative breast cancer (TNBC) cell lines, MDA-MB-231 and MDA-MB-157, when treated in low extracellular zinc conditions compared to higher extracellular zinc conditions (Woyciehowsky et al., 2025). This observation was made after a series of resazurin assays were carried out on various breast cancer cell lines including a non-transformed breast cell line MCF10a. A similar number of cells were plated in a 96-well plate and were treated for 48 hours in minimal media (MM) conditions supplemented with either tris(2-pyridylmethyl)amine (TPA) to produce a zinc deficient (ZD) environment or $ZnCl_2$ to produce a zinc rich (ZR) environment. After this period, resazurin was added to cells which can be converted to a fluorescently active metabolite, resorufin, by metabolically active mitochondria. The fluorescence intensity in a given well was used to compare the metabolic activity of the different cancer cell lines after the 48-hour treatment to the TPA or ZnCl2-supplemented media conditions. What this assay could not determine was whether the lower metabolic activity was due to cells entering a state of quiescence (departure from the cell cycle) or changes in cell viability i.e. cell death. A series of live/dead assays were performed on these breast cancer cell lines after a 48-hour treatment to TPA (ZD) and $ZnCl_2$ (ZR) supplemented MM to determine a change in cell viability; my research specifically focused on the TNBC cell lines, MDA-MB-231 and MDA-MB-157.

The live/dead assay data would suggest that TNBC cells respond to the amount of zinc in their environment differently than healthy epithelial breast cells. The MDA-MB-231 and MDA-MB-157 cell lines show a higher percentage of dead cells in the low extracellular zinc conditions

(2ZD) compared to the MCF10A cell line (**Fig. 1**). In contrast, the MCF10A cell line showed a higher fraction of dead cells in the high extracellular zinc conditions, for which the MDA-MB-231 and MDA-MB-157 cell line showed little to no change in viability compared to the unaltered minimal media condition (MM). Although cell death was observed, it was unclear whether the cells were dying via a necrotic or apoptotic mechanism, so apoptosis assays were performed on these cell lines.

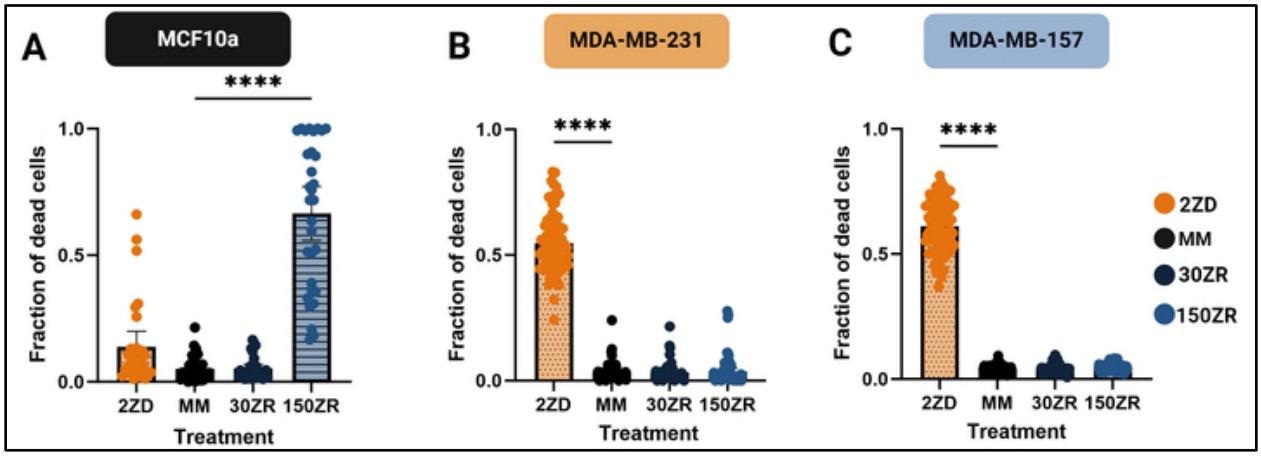

Figure 1: Changes in triple-negative breast cancer (TNBC) cell viability suggest a strong dependency on zinc. Live/dead assay results for MCF10a (A), MDA-MB-231 (B), and MDA-MB-157 (C) treated in a series of supplemented minimal media conditions for 48 hours: 2 µM TPA (2ZD), no supplement minimal media (MM), 30 µM $ZnCl_2$ (30ZR), and 150 µM $ZnCl_2$ (150ZR). All data was collected in n = 2 biological replicates with a statistical analysis performed by Brown-Forsythe and Welch ANOVA with Dunnett's T3 multiple comparison test: $^{****}p < 0.0001$. Each dot represents the fraction of dead cells in one well of a 96-well plate. For (A) MCF10A, contributions for data collection goes to the Palmer lab.

Apoptosis assay:

After discovering that the MDA-MB-231 cells die in low extracellular zinc conditions, unlike the non-transformed MCF10a cell line, it remained unclear the mechanism of death carried out by the cells, whether it be apoptotic or necrotic. To determine this, we began optimizing an apoptosis assay, as we hypothesize that the lack of zinc can increase the susceptibility of the MDA-MB-231 cells to enter apoptosis. There was also interest in determining the mechanism of cell death occurring in the noncancerous MCF10A cells when treated in high concentrations of extracellular zinc. To determine this, both cell lines were treated in a zinc deficient (3ZD) condition, 3 μM TPA supplemented MM, and a zinc rich (150ZR) condition, 150 μM $ZnCl_2$ supplemented MM, as these represented the two extremes of interest for these cell lines. The positive control for the assay is the addition of a topoisomerase I inhibitor, camptothecin, which induces apoptosis through DNA damage, and the negative control is MM with no TPA or $ZnCl_2$ supplement to represent an unaltered extracellular zinc condition.

The first step to finalizing the apoptosis assay data from the cytometer is to gate the untreated cells to exclude small particles and doublets of cells (**Fig. 2)**. The plot on the left is a forward scatter area (FSC-A) vs. a side scatter area (SSC-A); the red outline (P1) is the first gate selected for viable and necrotic/apoptotic cells. The plot on the right is forward scatter height (FSC-H) vs. FSC-A; the red outline (P2) is the second gate inside P1 selecting for single cells. The untreated control (negative control with no addition of Alexa 647 or SYTOX green) is used for this gating process. After this gating process, the SYTOX green and Alexa 647 histograms are used from single fluorophore controls to determine whether there is bleedthrough between the two probes used for the assay

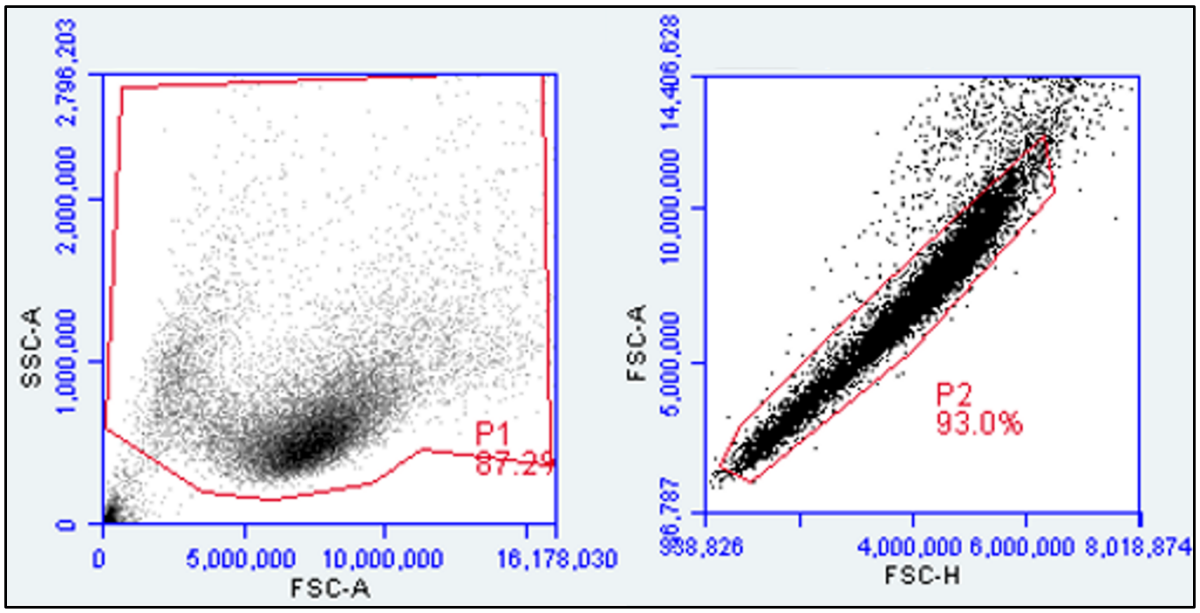

Figure 2: Forward scatter (FSC) and side scatter (SSC) area and height plots are used to select particles of the correct size and shape.

Single fluorophore controls were compared to an untreated control to determine whether bleedthrough occurred between the two probe's emission spectra used for this assay. There were two biological replicates of single fluorophore controls treated in MM conditions to check for bleedthrough between the channels of the dyes (**Fig. 3**). The SYTOX green histograms from the Alexa 647 single control are outlined in red and the Alexa 647 histograms from the SYTOX green single control are outlined in green. These are compared to an untreated cell population with no addition of either fluorophore outlined in black. Since there was no bleedthrough between the two probes' emission spectra, apoptosis assays were performed on the MDA-MB-231 cell line.

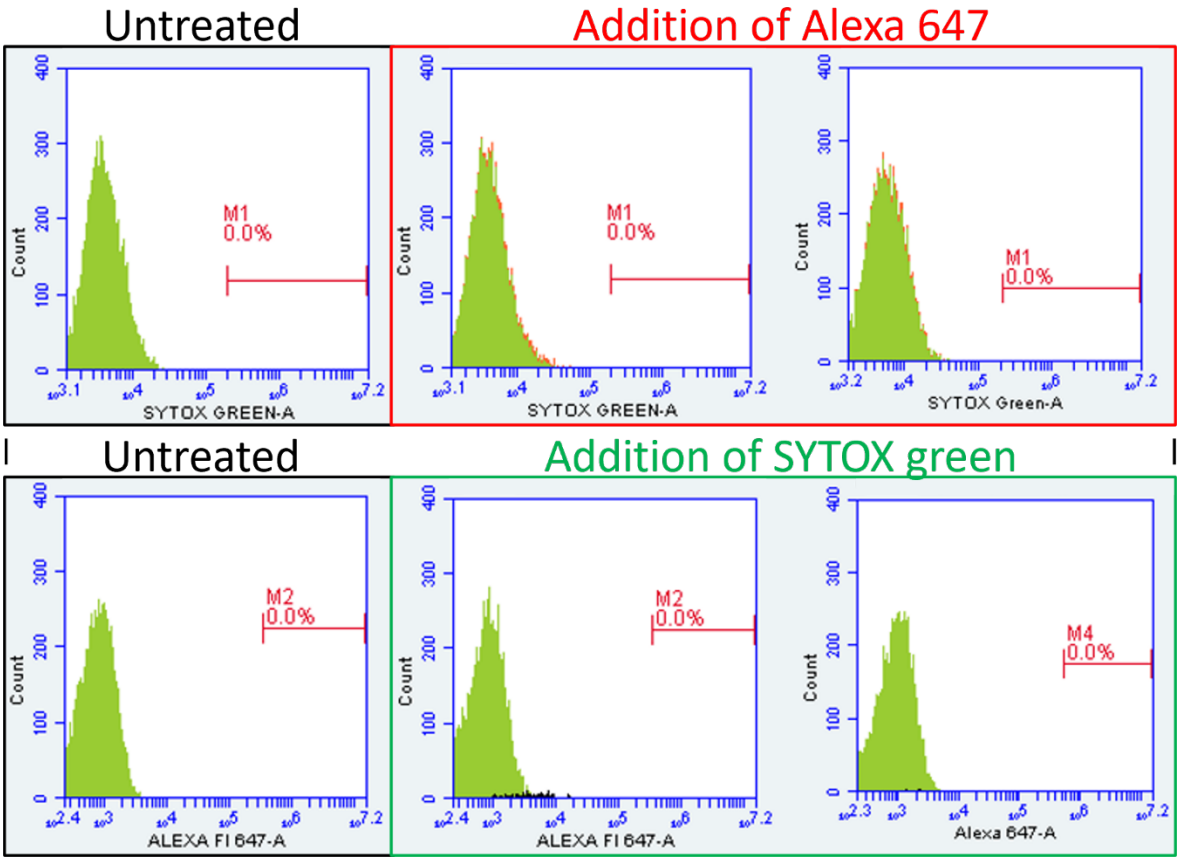

Figure 3: Single fluorophore control treatments of Alexa 647 and SYTOX green ensure no bleedthrough between channels of the dyes. These are histograms of the fluorophore intensity per cell count of each single control compared to the untreated control which received no fluorophore; black outline (SYTOX green and Alexa 647 histograms from the untreated control), red outline (SYTOX green histogram from the Alexa 647 control), and green outline (Alexa 647 histogram from the SYTOX green control).

Data from the apoptosis assay performed on the MDA-MB-231 cell line suggest that zinc-deficient conditions induce apoptosis and necrosis. Data collected on the MDA-MB-231 cell line are represented by 2D plots of Alexa 647 vs. SYTOX green intensities (**Fig. 4**). There were

higher percentages of early apoptotic cells when treated in the zinc-deficient condition (3ZD) after 48 hours compared to 24 hours, however, there was a decrease in the percent of late apoptotic cells after this longer incubation period, and instead, a higher percent of necrotic cells was present. The positive control (18 μM camptothecin) appeared to induce more necrosis during the longer 48-hour incubation period compared to the 24-hour incubation period, with small changes in late and early apoptotic cell percentages. Overall, the 3ZD condition induces more early necrosis and early/late apoptosis in the MDA-MB-231 cells compared to the positive control after both 24-hour and 48-hour incubation periods. As predicted from the live/dead assays, the MDA-MB-231 cells survived in the zinc-rich (150ZR) condition with negligible changes in apoptotic and necrotic cell percentages compared to the negative control in both incubation periods. The apoptosis assays were then performed on the MCF10A cell line to determine the mechanism of cell death observed in the high extracellular zinc conditions from the live/dead assays.

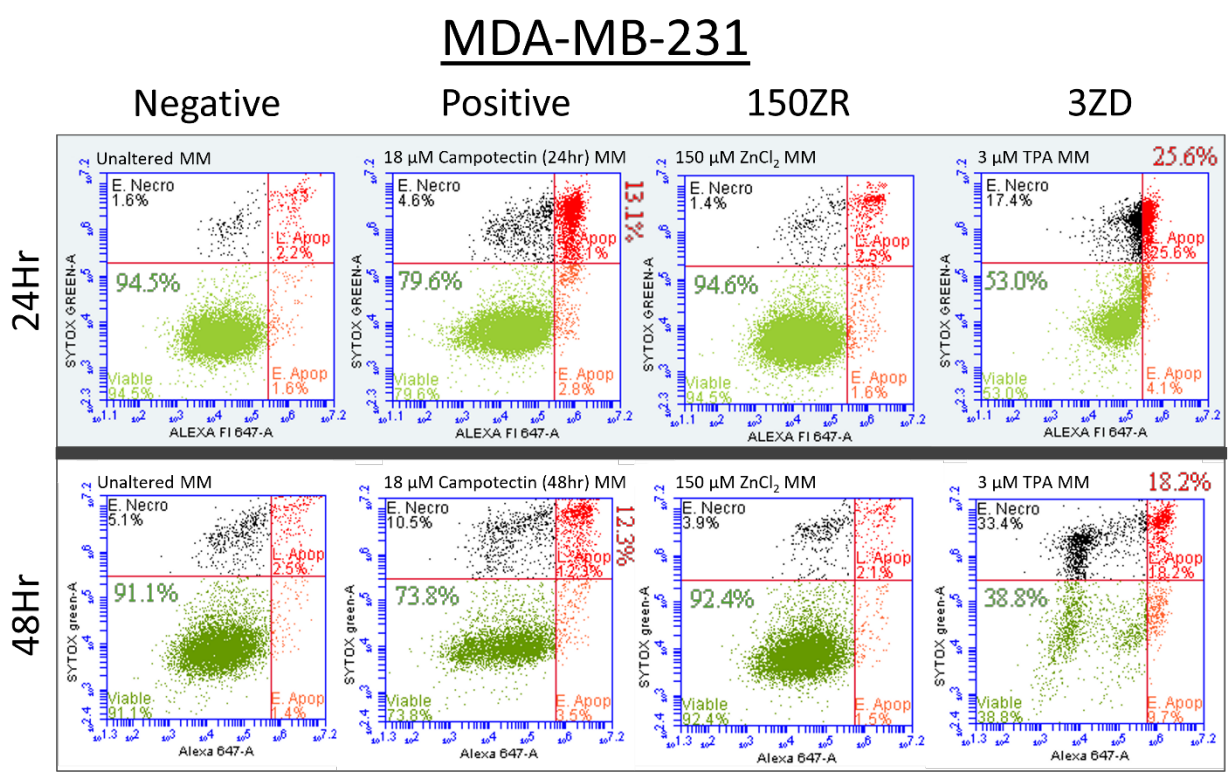

Figure 4: The percentage of both apoptotic and necrotic MDA-MB-231 cells is higher when treated in a zinc-deficient condition (3ZD) for a longer incubation period. The controls and conditions are noted above the plots and the incubation periods are noted to the left of the plots. Directly above each plot, the specific concentrations of reagents supplemented to minimal media (MM) for a control or condition are given: Negative (unaltered MM), positive (18 µM camptothecin supplemented MM), 150ZR (150 µM $ZnCl_2$ supplemented MM), and 3ZD (3 µM TPA supplemented MM). Each plot is separated into four quadrants: Viable (green), early apoptotic (E. Apop, orange), late apoptotic/necrotic (L. Apop, red), and early necrotic (E. Necro, black).

Data collected from the apoptosis assays performed on the MCF10A cell line suggest that zinc-rich conditions induce a mainly apoptotic mechanism of death. Data on the MCF10A cell line are also represented by 2D plots of Alexa 647 vs. SYTOX green intensities (**Fig. 5**). There were higher percentages of early and late apoptosis in MCF10A cells incubated in high zinc conditions (150ZR) compared to the negative control after both 24-hour and 48-hour incubation periods. Zinc deficient conditions (3ZD) also induced higher percentages of early and late apoptosis compared to the negative control after 24 hours, however, there were higher percentages of late apoptosis in the negative control after 48 hours. The negative control from the 48-hour incubation assay had a population of early necrotic and late apoptotic cells that had not been present in the 24-hour incubation assay which may account for the higher percentage of late apoptotic cells compared to the 3ZD condition. The 48-hour incubation period induced a higher percentage of early necrotic cells across all conditions and controls compared to the 24-hour incubation period, with an exception for the positive control which had low percentages of early necrotic and late apoptotic cells in both incubation periods. To compare the results from the MDA-MB-231 and MCF10A cell lines, a series of bar graphs were created to represent the percentage of cells that appear in each quadrant of the 2D plots on a linear scale.

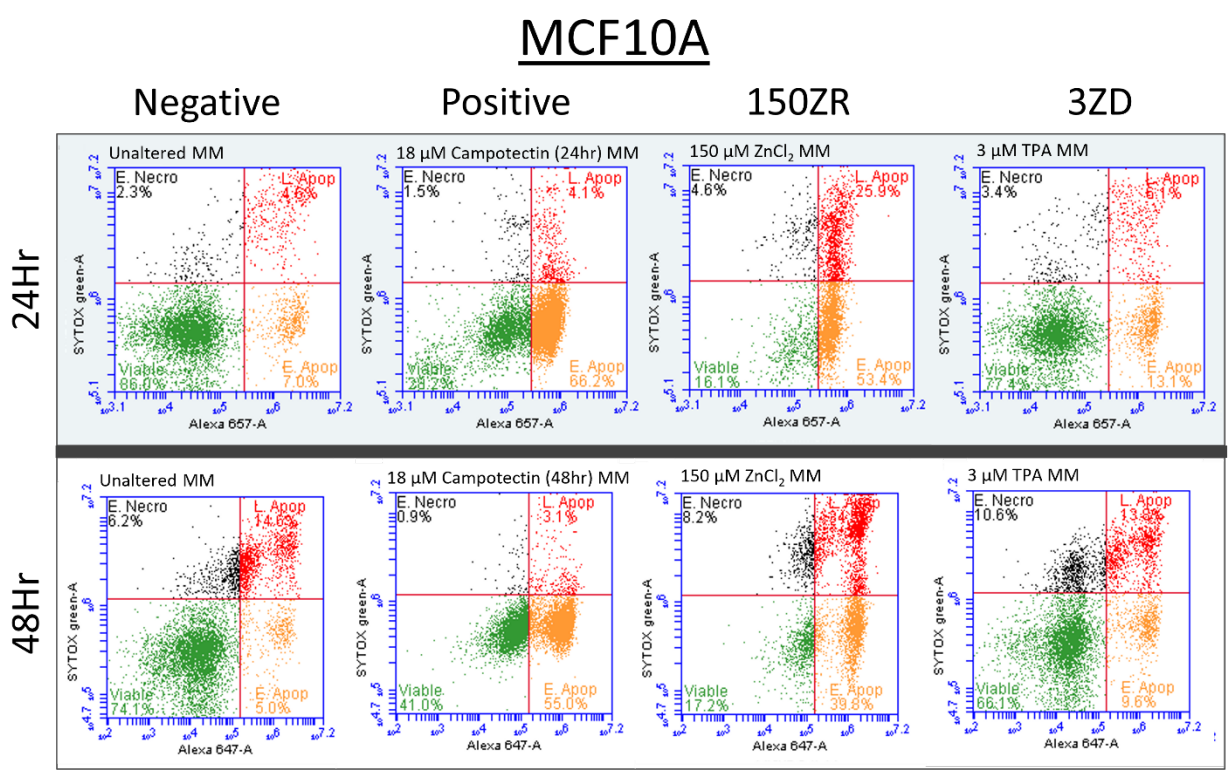

Figure 5: Apoptosis assays suggest death in MCF10A cells follows an apoptotic and necrotic mechanism in high zinc conditions. The controls and conditions are noted above the plots and the incubation periods are noted to the left of the plots. Directly above each plot, the specific concentrations of reagents supplemented to minimal media (MM) for a control or condition are given: Negative (unaltered MM), positive (18 µM camptothecin supplemented MM), 150ZR (150 µM $ZnCl_2$ supplemented MM), and 3ZD (3 µM TPA supplemented MM). Each plot is separated into four quadrants: Viable (green), early apoptotic (E. Apop, orange), late apoptotic/necrotic (L. Apop, red), and early necrotic (E. Necro, black).

MDA-MB-231 shows higher resistance to apoptosis compared to MCF10A cells when faced with apoptotic-inducing factors, and instead, more necrosis is observed. After compiling the apoptosis assay data onto bar graphs, there were about 10-fold more early necrotic, 11-fold more late apoptotic, and twice as many early apoptotic MDA-MB-231 cells grown in the 3ZD condition compared to the negative control after 24 hours (**Fig. 6A**). There was a change from 17.4% to 33.4% early necrotic cells, 25.6% to 18.2% late apoptotic cells, and 4.1% to 9.7% early apoptotic cells when incubated in 3ZD for 48 hours compared to 24 hours (**Fig. 6B**). There were minimal changes in % viable, necrotic, and apoptotic MDA-MB-231 cells treated in the 150ZR condition compared to the negative control (**Fig. 6A, B**). There were about 6-fold more late apoptotic and 8-fold more early apoptotic MCF10A cells treated in the 150ZR condition compared to the negative control with minimal differences in the percentage of necrotic cells. In the 3ZD condition, there were about twice as many early apoptotic MCF10A cells compared to the negative control (**Fig. 6C**). There was a change from 53.4% to 39.8% early apoptotic, 25.6% to 34.8% late apoptotic, and 4.6% to 8.2% early necrotic MCF10A cells when treated in 150ZR for 48 hours compared to 24 hours. In the 3ZD there were about twice as many more late apoptotic and 3-fold more necrotic MCF10A cells after this longer incubation period (**Fig. 6D**). Although further optimization of the assay is required for the MDA-MB-231 cell line, important insight on the mechanism of cell death observed from the live/dead assays have been made with the data collected from the apoptosis assays so far.

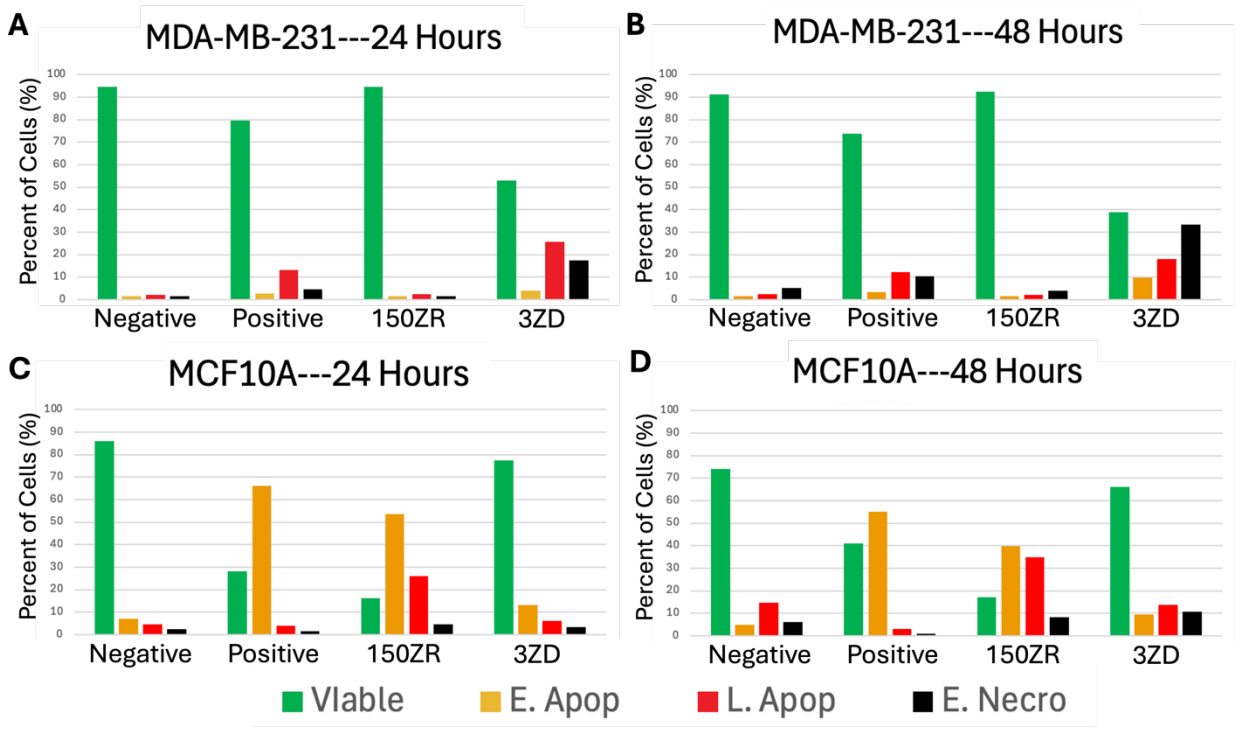

Figure 6: Results from apoptosis assay suggest MDA-MB-231 cells have an overall higher resistance to apoptosis compared to MCF10A cells. Data from the apoptosis assays performed on the MDA-MB-231 and MCF10A cell lines are compiled into the bar graphs above; **A)** MDA-MB-231 after 24-hour incubation, **B)** MDA-MB-231 after 48-hour incubation, **C)** MCF10A after 24-hour incubation, and **D)** MCF10A after 48-hour incubation. The bar graphs represent the incubation conditions vs. percentage of cells present in each quadrant from the 2D plots in **Figure 4** and **Figure 5**; viable cells (green), early apoptotic cells (orange), late apoptotic/necrotic cells (red), and early necrotic cells (black). Only 1 biological replicate, so no statistical analysis performed.

---------- Discussion ----------

Live/dead and apoptosis assay:

Zinc has been shown to play a major role in maintaining the health of a living organism through proper enzymatic function (McCall et al., 2000), growth and development (Maret, 2013), and gene regulation (Jackson et al., 2008). With a growing understanding of the importance of zinc, a meta-analysis showed increased concentrations of zinc present in breast cancer tumors (Jouybari et al., 2019). Although zinc appeared to be elevated in breast tumors, there had been conflicting information as to the levels of zinc present across multiple subtypes of breast cancer that a recent study in the lab addressed utilizing a Fluorescence Resonance Energy Transfer (FRET)-based biosensor ZapCV2 that increases in fluorescence upon binding of free Zn^{2+} ions. From this study, triple-negative breast cancer (TNBC) cell lines had the highest levels of free zinc among other subtypes of breast cancer including healthy epithelial breast cells (Woyciehowsky et al., 2025). The study also showed decreased mitochondrial activity (cell count) across multiple subtypes of breast cancer when treated in zinc-deficient conditions, including the TNBC subtype, through resazurin assays. However, these assays did not provide insight into whether the decreased mitochondrial activity was due to lower cell counts caused by cell death or lower cell counts due to a lack of proliferation by entering a state of quiescence. To determine this, live/dead assays were performed on the TNBC cell lines to compare to the live/dead assays already performed on the healthy epithelial breast cells in the lab, and then apoptosis assays were performed to determine the mechanism of death observed from the live/dead assays.

Results from the live/dead assays performed on the MDA-MB-231 and MDA-MB-157 cell lines provided important findings with respect to the viability of TNBC cell lines when treated in zinc-deficient conditions. From the live/dead assays, both MDA-MB-231 and MDA-MB-157 cell lines showed an increased fraction of dead cells after treatment in zinc-deficient conditions in contrast to MCF10A cells that were mostly viable, conversely, there was an increase in the fraction of dead MCF10A cells after treatment in zinc-rich conditions that the MDA-MB-231 and MDA-MB-157 cell lines appeared to be highly resistant to (**Fig. 1**). TNBC cells appear to have a higher dependency for zinc as they show lower viability in zinc-deficient conditions, yet they have a higher resistance to cell death in zinc-rich conditions compared to healthy epithelial breast cells that show lower viability in these zinc-rich conditions. This result was initially unexpected as the MCF10A cell line did not show a decrease in viability when treated in the zinc-deficient condition before running the assay on the TNBC cell lines.

Interested in the mechanism of cell death observed from the live/dead assay results on the MDA-MB-231 and MCF10A cell lines, apoptosis assays were performed on these cells after treatment with zinc-deficient and zinc-rich media conditions. Since the goal of the assay was to detect viable, apoptotic, and necrotic cells, the gating process only excludes small particles and possible doublets of cells (**Fig. 2**). To distinguish the viable, apoptotic, and necrotic cells from each other, the assay utilizes two fluorescent probes, Alexa Fluor 647 and SYTOX green. Alexa 647, which conjugates to Annexin V, binds to an inner membrane phospholipid, phosphatidylserine, present when the membrane of the cell becomes inverted during apoptosis. SYTOX green, which is membrane impermeable, stains the nucleus of a cell with a compromised membrane during necrosis. Since two probes are used in this assay, single fluorophore controls were created to

determine whether there was bleedthrough occurring between the probe's emission spectra. After performing two assays with the single fluorophore controls, there was no bleedthrough observed (**Fig. 3**) and the probes could be used together for the duration of the assays. The assays are performed after 24- and 48-hour incubation periods as studies have shown that the timeframe for apoptosis can vary based on cell type (Bhola & Simon, 2009) and among cells from the same population (Cano-González et al., 2018). We predict that the MDA-MB-231 cells will be more susceptible to apoptosis in zinc-deficient conditions since zinc is observed to inhibit Caspase 3 (Truong-Tran et al., 2001) and we were also interested in the mechanism of death observed in MCF10A cells after treatment to zinc-rich conditions.

Although further optimization of the assay is required, current data provides important insight into the mechanism of death observed in the MDA-MB-231 cell line when treated in zinc-deficient conditions and the MCF10A cell line when treated in zinc-rich conditions. After treatment in the zinc-deficient conditions, both apoptosis and necrosis were observed in the MDA-MB-231 cell line as there are higher percentages of early necrotic and early/late apoptotic cells compared to the cells treated in the unaltered zinc conditions, even more prominent after the longer incubation period (**Fig. 4**). The increase in apoptosis aligned with our initial prediction, however, there was also an increase in necrosis which had not been predicted. Alternatively, after treatment in the zinc-rich media conditions, mainly apoptosis was observed in the MCF10A cells as there were higher percentages of early/late apoptotic cells compared to cells treated in the unaltered zinc conditions with less prominent changes in the percentage of early necrotic cells (**Fig. 5**). The data from the MDA-MB-231 and MCF10A assays were compiled into a series of graphs that represented the percentages of cell that were either viable, early necrotic, early

apoptotic, or late apoptotic in a given media condition after the 24- and 48-hour incubation periods. From this compiled data, the MDA-MB-231 cells showed an overall higher resistance to apoptosis compared to the MCF10A cell line and higher percentages of necrosis were observed in both cell lines after the longer incubation period (**Fig. 6**). This resistance to apoptosis observed in the MDA-MB-231 cell line was not unexpected as a recent study showed that TNBCs have a high resistance to apoptosis through elevation of Bcl-2, an anti-apoptotic protein (Nocquet et al., 2024).

Overall, the live/dead and apoptosis assays suggest that TNBCs have a strong dependency on zinc, and without it, they become both necrotic and apoptotic, whereas zinc-rich conditions induce mainly apoptosis in healthy epithelial breast cells. Until now, there was little information about the effects on TNBC cells treated with zinc-deficient conditions, however, a study presented similar results when treating MDA-MB-231 cells to zinc-rich conditions that showed little changes in viability, with the exception of a high concentration of $ZnSO_4$ (200 μM) that significantly increased apoptosis (Wang et al., 2015). There was also little information about the effects of zinc on apoptosis in healthy epithelial breast cells. One study measured the viability of MCF10A cells with the addition of zinc bound to a porphyrin ring, however, the viability of the cells decreased similarly to the addition of the porphyrin ring without zinc bound and the observed mechanism of cell death from this study was mainly necrotic (25 - 57%) compared to apoptotic (2 -3%) with and without zinc bound (Soriano et al., 2017).

Future directions:

For future directions for this project, we would like to optimize this assay for the MDA-MB-231 cell line by incubating the cells in the probes for the shorter period that was used to collect data on the MCF10A cell line. The reason for this change was from research presented by Rich Hastings at KU Medical Center that suggested an overly long incubation period in the annexin-binding solution can lead to unwanted binding interactions with the Annexin V protein, and other iterations of the assay added the SYTOX green probe only 5 min before imaging. There is also a low percentage of apoptosis induced in the MDA-MB-231 cell line in general compared to the MCF10A cell line and a more recent study that may be worth exploring utilized a non-selective kinase inhibitor, staurosporine (STS), as a positive control for an Annexin V assay performed on MDA-MB-231 cells. In the study, 0.75 μM STS treatment for 96 hours produced 56.3% early apoptotic cells compared to 1.16% in the negative control (Hastings & Kenealey, 2017). We predict that utilizing a higher concentration of this kinase inhibitor could produce similar percentages of early apoptotic cells in a shorter period of time that aligns with the 24- and 48-hour incubation periods of my apoptosis assay.

After optimizing the assay on the MDA-MB-231 and MCF10A cells, we would like to then repeat these assays on more breast cancer cell lines. This could provide valuable insight into the similarities and differences in zinc's role in cell death across multiple subtypes of breast cancers.

Depending on the mechanism of death observed, it would be worth exploring possible apoptotic proteins that zinc may be activating/inhibiting to induce possible apoptotic events in these cells.

Acknowledgements:

First, I would like to thank Dr. Amy Palmer for the opportunity to carry out and present research during my undergraduate term at CU Boulder. I would also like to thank Sam Holtzen and Ananya Rakshit for their guidance throughout these experiments, and the rest of the Palmer lab for cultivating a warm, welcoming presence throughout my time conducting research in the lab.

Finally, I would like to thank my family for their relentless support, always giving me the motivation I need to keep working towards my goals in life. As a first-generation college student in my family, this was a new adventure for all of us.

References:

Alberts, B., Bray, D., Lewis, J., Raff, M., Roberts, K., & Watson, J. D. (1994). *Molecular biology of the cell* (Vol. 3, pp. 966–996). New York: Garland.

American Cancer Society. (2024, January 12). *Key Statistics for Breast Cancer*. American Cancer Society. https://www.cancer.org/cancer/types/breast-cancer/about/how-common-is-breast-cancer.html

Anandakrishnan, R., Varghese, R. T., Kinney, N. A., & Garner, H. R. (2019). Estimating the Number of Genetic Mutations (hits) Required for Carcinogenesis Based on the Distribution of Somatic Mutations. *PLOS Computational Biology*, *15*(3), e1006881. https://doi.org/10.1371/journal.pcbi.1006881

Bauer, K. R., Brown, M., Cress, R. D., Parise, C. A., & Caggiano, V. (2007). Descriptive analysis of estrogen receptor (ER)-negative, progesterone receptor (PR)-negative, and HER2-negative invasive breast cancer, the so-called triple-negative phenotype. *Cancer*, *109*(9), 1721–1728. https://doi.org/10.1002/cncr.22618

Benz, C. C. (2008). Impact of aging on the biology of breast cancer. *Critical Reviews in Oncology/Hematology*, *66*(1), 65–74. https://doi.org/10.1016/j.critrevonc.2007.09.001

Bhola, P. D., & Simon, S. M. (2009). Determinism and divergence of apoptosis susceptibility in mammalian cells. Journal of Cell Science, 122(23), 4296–4302. https://doi.org/10.1242/jcs.055590

Burkhalter, M. D., Rudolph, K. L., & Sperka, T. (2015). Genome instability of ageing stem

cells—Induction and defence mechanisms. *Ageing Research Reviews*, *23*, 29–36. https://doi.org/10.1016/j.arr.2015.01.004

Cano-González, A., Mauro-Lizcano, M., Iglesias-Serret, D., Gil, J., & López-Rivas, A. (2018). Involvement of both caspase-8 and Noxa-activated pathways in endoplasmic reticulum stress-induced apoptosis in triple-negative breast tumor cells. Cell Death & Disease, 9(2). https://doi.org/10.1038/s41419-017-0164-7

Çelik, A., Acar, M., Erkul, C. M., & Gunduz, E. G. and M. (2015). Relationship of Breast Cancer with Ovarian Cancer. *A Concise Review of Molecular Pathology of Breast Cancer*. https://doi.org/10.5772/59682

Collaborative Group on Hormonal Factors in Breast Cancer. (2001). Familial breast cancer: collaborative reanalysis of individual data from 52 epidemiological studies including 58 209 women with breast cancer and 101 986 women without the disease. *The Lancet*, *358*(9291), 1389–1399. https://doi.org/10.1016/s0140-6736(01)06524-2

Crick, F. (1970). Central Dogma of Molecular Biology. *Nature*, *227*(5258), 561–563. https://doi.org/10.1038/227561a0

Drake, J. W., Charlesworth, B., Charlesworth, D., & Crow, J. F. (1998). Rates of Spontaneous Mutation. *Genetics*, *148*(4), 1667–1686. https://doi.org/10.1093/genetics/148.4.1667

Endogenous Hormones and Breast Cancer Collaborative Group. (2013). Sex hormones and risk of breast cancer in premenopausal women: a collaborative reanalysis of individual participant data from seven prospective studies. *The Lancet Oncology*, *14*(10), 1009–1019. https://doi.org/10.1016/s1470-2045(13)70301-2

Fanzo, J. C., Reaves, S. K., Cui, L., Zhu, L., & Lei, K. Y. (2002). p53 protein and p21 mRNA levels and caspase-3 activity are altered by zinc status in aortic endothelial cells.

American Journal of Physiology-Cell Physiology, *283*(2), C631–C638. https://doi.org/10.1152/ajpcell.00248.2001

Farquharson, M. J., A. Al-Ebraheem, K Geraki, Leek, R., & Harris, A. L. (2009). Zinc presence in invasive ductal carcinoma of the breast and its correlation with oestrogen receptor status. *Physics in Medicine and Biology*, *54*(13), 4213–4223. https://doi.org/10.1088/0031-9155/54/13/016

Fuchs, E. (2009). The Tortoise and the Hair: Slow-Cycling Cells in the Stem Cell Race. *Cell*, *137*(5), 811–819. https://doi.org/10.1016/j.cell.2009.05.002

Gonzalez-Angulo, A. M., Timms, K. M., Liu, S., Chen, H., Litton, J. K., Potter, J., Lanchbury, J. S., Stemke-Hale, K., Hennessy, B. T., Arun, B. K., Hortobagyi, G. N., Do, K.-A. ., Mills, G. B., & Meric-Bernstam, F. (2011). Incidence and Outcome of BRCA Mutations in Unselected Patients with Triple Receptor-Negative Breast Cancer. *Clinical Cancer Research*, *17*(5), 1082–1089. https://doi.org/10.1158/1078-0432.ccr-10-2560

Hanahan, D., & Weinberg, R. A. (2000). The Hallmarks of Cancer. *Cell*, *100*(1), 57–70. https://doi.org/10.1016/s0092-8674(00)81683-9

Hastings, J., & Kenealey, J. (2017). Avenanthramide-C reduces the viability of MDA-MB-231 breast cancer cells through an apoptotic mechanism. *Cancer Cell International*, *17*(1). https://doi.org/10.1186/s12935-017-0464-0

Hayflick, L., & Moorhead, P. S. (1961). The serial cultivation of human diploid cell strains. *Experimental Cell Research*, *25*(3), 585–621. https://doi.org/10.1016/0014-4827(61)90192-6

Hill, D. A., Prossnitz, E. R., Royce, M., & Nibbe, A. (2019). Temporal trends in breast cancer survival by race and ethnicity: A population-based cohort study. *PLOS ONE*, *14*(10),

e0224064. https://doi.org/10.1371/journal.pone.0224064

Hirsch, T., Marchetti, P., Susin, S. A., Dallaporta, B., Zamzami, N., Marzo, I., Geuskens, M., & Kroemer, G. (1997). The apoptosis-necrosis paradox. Apoptogenic proteases activated after mitochondrial permeability transition determine the mode of cell death. *Oncogene*, *15*(13), 1573–1581. https://doi.org/10.1038/sj.onc.1201324

Jouybari, L., Kiani, F., Akbari, A., Sanagoo, A., Sayehmiri, F., Aaseth, J., Chartrand, M. S., Sayehmiri, K., Chirumbolo, S., & Bjørklund, G. (2019). A meta-analysis of zinc levels in breast cancer. *Journal of Trace Elements in Medicine and Biology*, *56*, 90–99. https://doi.org/10.1016/j.jtemb.2019.06.017

Kerr, J. F. R., Wyllie, A. H., & Currie, A. R. (1972). Apoptosis: A Basic Biological Phenomenon with Wideranging Implications in Tissue Kinetics. *British Journal of Cancer*, *26*(4), 239–257. https://doi.org/10.1038/bjc.1972.33

Koopman, G., Reutelingsperger, C., Kuijten, G., Keehnen, R., Pals, S., & van Oers, M. (1994). Annexin V for flow cytometric detection of phosphatidylserine expression on B cells undergoing apoptosis. *Blood*, *84*(5), 1415–1420. https://doi.org/10.1182/blood.v84.5.1415.1415

Libby, E., & Ratcliff, W. C. (2014). Ratcheting the evolution of multicellularity. *Science*, *346*(6208), 426–427. https://doi.org/10.1126/science.1262053

Liu, S., Xu, H., Feng, Y., Kahlert, U. D., Du, R., Angela, L., Xu, K., Shi, W., & Meng, F. (2023). Oxidative stress genes define two subtypes of triple-negative breast cancer with prognostic and therapeutic implications. *Frontiers in Genetics*, *14*. https://doi.org/10.3389/fgene.2023.1230911

Lo, M. N., Damon, L. J., Wei Tay, J., Jia, S., & Palmer, A. E. (2020). Single cell analysis reveals

multiple requirements for zinc in the mammalian cell cycle. *ELife*, *9*, e51107. https://doi.org/10.7554/eLife.51107

Lowe, N. M., Hall, A. G., Broadley, M. R., Foley, J., Boy, E., & Bhutta, Z. A. (2024). Preventing and Controlling Zinc Deficiency Across the Life Course: A Call to Action. *Advances in Nutrition*, *15*(3), 100181. https://doi.org/10.1016/j.advnut.2024.100181

Łukasiewicz, S., Czeczelewski, M., Forma, A., Baj, J., Sitarz, R., & Stanislawek, A. (2021). Breast cancer—epidemiology, Risk factors, classification, Prognostic markers, and Current Treatment Strategies—an Updated Review. *Cancers*, *13*(17), 4287. https://doi.org/10.3390/cancers13174287

Meacham, C. E., & Morrison, S. J. (2013). Tumour heterogeneity and cancer cell plasticity. *Nature*, *501*(7467), 328–337. https://doi.org/10.1038/nature12624

Mendiratta, G., Ke, E., Aziz, M., Liarakos, D., Tong, M., & Stites, E. C. (2021). Cancer gene mutation frequencies for the U.S. population. *Nature Communications*, *12*(1), 5961. https://doi.org/10.1038/s41467-021-26213-y

Mohammed, H., Russell, I. A., Stark, R., Rueda, O. M., Hickey, T. E., Tarulli, G. A., Serandour, A. A., Birrell, S. N., Bruna, A., Saadi, A., Menon, S., Hadfield, J., Pugh, M., Raj, G. V., Brown, G. D., D'Santos, C., Robinson, J. L. L., Silva, G., Launchbury, R., & Perou, C. M. (2015). Progesterone receptor modulates ERα action in breast cancer. *Nature*, *523*(7560), 313–317. https://doi.org/10.1038/nature14583

National Cancer Institute. (2015, April 29). *Surgery*. National Cancer Institute; Cancer.gov. https://www.cancer.gov/about-cancer/treatment/types/surgery

National Cancer Institute. (2024, May 9). *Cancer statistics*. National Cancer Institute. https://www.cancer.gov/about-cancer/understanding/statistics

Nocquet, L., Roul, J., Lefebvre, C. C., Duarte, L., Campone, M., Juin, P. P., & Frédérique Souazé. (2024). Low BCL-xL expression in triple-negative breast cancer cells favors chemotherapy efficacy, and this effect is limited by cancer-associated fibroblasts. *Scientific Reports*, *14*(1). https://doi.org/10.1038/s41598-024-64696-z

Norbury, C. J., & Hickson, I. D. (2001). Cellular responses to DNA damage. *Annual Review of Pharmacology and Toxicology*, *41*, 367–401. https://doi.org/10.1146/annurev.pharmtox.41.1.367

Rusch, P., Hirner, A. V., Schmitz, O., Kimmig, R., Hoffmann, O., & Diel, M. (2020). Zinc distribution within breast cancer tissue of different intrinsic subtypes. *Archives of Gynecology and Obstetrics*, *303*(1), 195–205. https://doi.org/10.1007/s00404-020-05789-8

Sender, R., Fuchs, S., & Milo, R. (2016). Revised Estimates for the Number of Human and Bacteria Cells in the Body. *PLOS Biology*, *14*(8), e1002533. https://doi.org/10.1371/journal.pbio.1002533

Sender, R., & Milo, R. (2021). The distribution of cellular turnover in the human body. *Nature Medicine*, *27*(1), 45–48. https://doi.org/10.1038/s41591-020-01182-9

Sergina, N. V., & Moasser, M. M. (2007). The HER family and cancer: emerging molecular mechanisms and therapeutic targets. *Trends in Molecular Medicine*, *13*(12), 527–534. https://doi.org/10.1016/j.molmed.2007.10.002

Shay, J. W., & Wright, W. E. (2000). Hayflick, his limit, and cellular ageing. *Nature Reviews Molecular Cell Biology*, *1*(1), 72–76. https://doi.org/10.1038/35036093

Soriano, J., Mora-Espí, I., Alea-Reyes, M. E., Pérez-García, L., Barrios, L., Ibáñez, E., & Nogués, C. (2017). Cell Death Mechanisms in Tumoral and Non-Tumoral Human Cell

Lines Triggered by Photodynamic Treatments: Apoptosis, Necrosis and Parthanatos. Scientific Reports, 7(1). https://doi.org/10.1038/srep41340

Sunderman FW. (1995). The influence of zinc on apoptosis. Annals of Clinical & Laboratory Science, 25(2), 134–142.

Swallow, D. M. (2003). Genetics of lactase persistence and lactose intolerance. *Annual Review of Genetics*, *37*(1), 197–219. https://doi.org/10.1146/annurev.genet.37.110801.143820

The American Cancer Society medical and editorial content team. (2020). *Breast Cancer Hormone Receptor Status | Estrogen Receptor*. American Cancer Society. https://www.cancer.org/cancer/types/breast-cancer/understanding-a-breast-cancer-diagnosis/breast-cancer-hormone-receptor-status.html?utm_source=chatgpt.com

Tomasetti, C., & Vogelstein, B. (2015). Variation in cancer risk among tissues can be explained by the number of stem cell divisions. *Science*, *347*(6217), 78–81. https://doi.org/10.1126/science.1260825

Vineis, P. (2003). Cancer as an evolutionary process at the cell level: an epidemiological perspective. *Carcinogenesis*, *24*(1), 1–6. https://doi.org/10.1093/carcin/24.1.1

Wang, Y., Zhao, W., Zheng, W., Mao, L., Lian, H., Hu, X., & Hua, Z. (2015). Effects of Different Zinc Species on Cellar Zinc Distribution, Cell Cycle, Apoptosis and Viability in MDAMB231 Cells. Biological Trace Element Research, 170(1), 75–83. https://doi.org/10.1007/s12011-015-0377-5

Watson, C. S., Jeng, Y., & Kochukov, M. Y. (2008). Nongenomic actions of estradiol compared with estrone and estriol in pituitary tumor cell signaling and proliferation. *The FASEB Journal*, *22*(9), 3328–3336. https://doi.org/10.1096/fj.08-107672

WATSON, J. D., & CRICK, F. H. C. (1953). Molecular Structure of Nucleic Acids: A Structure

for Deoxyribose Nucleic Acid. *Nature*, *171*(4356), 737–738. https://doi.org/10.1038/171737a0

Weissbein, U., Benvenisty, N., & Ben-David, U. (2014). Genome maintenance in pluripotent stem cells. *The Journal of Cell Biology*, *204*(2), 153–163. https://doi.org/10.1083/jcb.201310135

WHO. (2021). *World Cancer Day: know the facts – tobacco and alcohol both cause cancer*. World Health Organization. https://www.who.int/europe/news-room/03-02-2021-world-cancer-day-know-the-facts-tobacco-and-alcohol-both-cause-cancer?utm_source=chatgpt.com

Williams, A. B., & Schumacher, B. (2016). p53 in the DNA-Damage-Repair Process. *Cold Spring Harbor Perspectives in Medicine*, *6*(5), a026070. https://doi.org/10.1101/cshperspect.a026070

Wong, R. S. (2011). Apoptosis in cancer: from pathogenesis to treatment. *Journal of Experimental & Clinical Cancer Research*, *30*(1). https://doi.org/10.1186/1756-9966-30-87

Woyciehowsky, M., Larson, P., Stephan, A. R., Dandridge, S. L., Idonije, D., Berg, K. A., Lanthier, A., Acuna, S. A., Stites, S. W., Gebhardt, W. J., Holtzen, S. E., Rakshit, A., & Palmer, A. E. (2025). Systematic characterization of zinc in a series of breast cancer cell lines reveals significant changes in zinc homeostasis. *BioRxiv*. https://doi.org/10.1101/2025.01.11.632547

Zeinomar, N., Knight, J. A., Genkinger, J. M., Phillips, K.-A., Daly, M. B., Milne, R. L., Dite, G. S., Kehm, R. D., Liao, Y., Southey, M. C., Chung, W. K., Giles, G. G., McLachlan, S.-A., Friedlander, M. L., Weideman, P. C., Glendon, G., Nesci, S., Andrulis, I. L., Buys, S.

S., & John, E. M. (2019). Alcohol consumption, cigarette smoking, and familial breast cancer risk: findings from the Prospective Family Study Cohort (ProF-SC). *Breast Cancer Research*, *21*(1). https://doi.org/10.1186/s13058-019-1213-1

Zhao, X., Wei, C., Li, J., Xing, P., Li, J., Zheng, S., & Chen, X. (2017). Cell cycle-dependent control of homologous recombination. *Acta Biochimica et Biophysica Sinica*, *49*(8), 655–668. https://doi.org/10.1093/abbs/gmx055